1 **Inflammation induced by influenza virus impairs innate control of human pneumococcal**

2 **carriage**

3 Simon P. Jochems[1,§,*], Fernando Marcon[2,§], Beatriz F. Carniel[1], Mark Holloway[1], Elena Mitsi[1],

4 Emma Smith[1], Jenna F. Gritzfeld[1], Carla Solórzano[1], Jesús Reiné[1], Sherin Pojar[1], Elissavet

5 Nikolaou[1], Esther L. German[1], Angie Hyder-Wright[1,3], Helen Hill[1,3], Caz Hales[1,3], Wouter A.A de

6 Steenhuijsen Piters[4,5,6], Debby Bogaert[4,5,6], Hugh Adler[1], Seher Zaidi[1], Victoria Connor[1,3], Jamie

7 Rylance[1], Helder I. Nakaya[2,*], Daniela M. Ferreira[1,*]

8 **AFFILIATIONS**

9 [1] Department of Clinical Sciences, Liverpool School of Tropical Medicine, Liverpool, United

10 Kingdom

11 [2] Department of Clinical and Toxicological Analyses, School of Pharmaceutical Sciences,

12 University of São Paulo, SP, Brazil

13 [3] Royal Liverpool and Broadgreen University Hospital, Liverpool, United Kingdom

14 [4] Centre for Inflammation Research, University of Edinburgh, Edinburgh, United Kingdom

15 [5] Department of Paediatric Immunology and Infectious Diseases, Utrecht, The Netherlands

16 [6] Department of Medical Microbiology, University Medical Center Utrecht, The Netherlands

17

18 [§]both authors contributed equally to the work

19 [*]Corresponding authors: Dr. Simon P Jochems (simon.jochems@lstmed.ac.uk), Dr. Helder I

20 Nakaya (hnakaya@usp.br) and Dr Daniela M Ferreira (daniela.ferreira@lstmed.ac.uk)

21

Abstract

Secondary bacterial pneumonia following influenza infection is a significant cause of mortality worldwide. Upper respiratory tract pneumococcal carriage is important as both determinants of disease and population transmission. The immunological mechanisms that contain pneumococcal carriage are well-studied in mice but remain unclear in humans. Loss of this control of carriage following influenza infection is associated with secondary bacterial pneumonia during seasonal and pandemic outbreaks. We used a human type 6B pneumococcal challenge model to show that carriage acquisition induces early degranulation of resident neutrophils and recruitment of monocytes to the nose. Monocyte function associated with clearance of pneumococcal carriage. Prior nasal infection with live attenuated influenza virus induced inflammation, impaired innate function and altered genome-wide nasal gene responses to pneumococcal carriage. Levels of the cytokine IP-10 promoted by viral infection at the time of pneumococcal encounter was positively associated with bacterial density. These findings provide novel insights in nasal immunity to pneumococcus and viral-bacterial interactions during co-infection.

Main

Pneumonia is a major global health problem; it kills more children under 5 years of age than any other disease [1]. The burden of disease is aggravated by old age, chronic lung disease, immunosupression and viral co-infection. Secondary pneumonia following pandemic and seasonal influenza virus infection is a significant cause of mortality worldwide [2].

Nasopharyngeal carriage of *Streptococcus pneumoniae* (Spn, pneumococcus) is common with 40-95% of infants and 10-25% of adults colonised at any time [3]. Carriage is important as the pre-requisite of infection [4], the primary reservoir for transmission [5] and the predominant source of immunising exposure and immunological boosting in both children and adults [6,7].

Immune dysregulation caused by respiratory virus infection such as influenza leads to increased carriage density [8]. Increased carriage density has been associated with pneumonia incidence and

2

47   severity, as well as with within-household Spn transmission [5,9-11]. The mechanisms and markers

48   associated with this pathogen synergy have been difficult to study in human subjects due to the

49   rapid nature of the disease.

50   One safe way to simulate influenza infection in the nose is using Live Attenuated Influenza Vaccine

51   (LAIV), consisting of cold-adapted influenza viruses. LAIV has been shown to affect the

52   subsequent susceptibility to Spn and to lead to increased carriage density in murine models of

53   infection and in vaccinated children [12,13]. In a randomised controlled trial, we showed that LAIV

54   administration prior to Spn challenge led to 50% increase in Spn acquisition by molecular methods

55   as well as 10-fold increase in nasopharyngeal bacterial load [14].

56   In murine models of pneumococcal carriage, Th17-dependent recruitment of neutrophils and

57   monocytes to the nasopharynx mediates immunological control and clearance [15-17]. Influenza virus

58   infection promotes Type I interferons which interfere with recruitment of these phagocytes, while

59   IFN-□ is postulated to impair phagocytosis by macrophages through downregulation of the

60   scavenger receptor MARCO [18-20]. However, the precise immune mechanisms and gene regulators

61   involved in the control and clearance of pneumococcal carriage in humans have not been revealed

62   [21]. Moreover, how these mechanisms are altered during human influenza virus infection remains

63   largely unknown.

64   In recent years, systems biology approaches have allowed for the identification of immune

65   mechanisms associated with protection from infectious diseases and with robust immune

66   responses during vaccination [22-28]. Here, we applied systems biology to nasal samples collected in

67   the setting of human challenge with LAIV and Spn, to emulate nasal effects of influenza infection

68   on Spn carriage. We identified for the first time in humans the key cellular mechanisms that control

69   newly acquired pneumococcal carriage, and how they are disrupted following nasal influenza

70   infection.

71   **Results**

3

72 **LAIV-induced inflammation leads to increased pneumococcal carriage density and**

73 **acquisition**

74 In a double-blinded controlled randomized clinical trial, we administered LAIV (n=55) three days

75 prior to Spn inoculation (day 0). To verify the requisite topical application for an effect on

76 pneumococcal carriage, we administered tetravalent inactivated influenza vaccine (TIV) as a

77 control (n=62). LAIV infection led to transiently increased pneumococcal acquisition at day 2

78 (60.0% vs 40.3% by molecular methods in LAIV vs control groups, respectively) [14]. LAIV also

79 increased Spn carriage density in the first 14 days following pneumococcal inoculation (Fig S1 and

80 [14]). We collected a series of nasal micro-biopsies and nasal lining fluid throughout the study to

81 assess ongoing cellular and cytokine responses. Participants were grouped in those who did not

82 become colonized following Spn challenge (carriage-) and those who did (carriage+), as

83 determined by classical microbiology (Fig 1a). To investigate whether LAIV-induced immune

84 responses were associated with a predisposition to pneumococcal carriage, we measured levels of

85 30 cytokines in nasal lining fluid (Fig 1b). At day 0, directly prior to Spn inoculation, LAIV

86 significantly increased levels of twenty cytokines after multiple testing correction, including IP-10,

87 TNF-α, IL-10, IFN-□ and IL-15 (Fig 1b and Table S1). In contrast, the control group did not show

88 any significant increase in cytokine response at day 0. Following Spn inoculation, Spn carriage in

89 the absence of LAIV was associated with increased levels of EGF at day 2 (p = 0.023) and

90 decreased levels of IL-1RA at day 9 post Spn inoculation (p = 0.027) compared to baseline, neither

91 of which remained significant after multiple testing correction. No other cytokines, including IL-17A

92 or MCP-1, were significantly altered by carriage alone (Fig 1b).

93 Even before bacterial inoculation, nasal inflammatory responses to LAIV differed between those

94 who went on to become carrier and those who were protected from carriage (Fig 1c). In particular,

95 IL-10 was increased more in LAIV-vaccinated subjects who did not acquire Spn following

96 inoculation (5.8-fold increase, p = 0.0097) than in those who became carriers following inoculation

97 (2.0-fold increase, p = 0.073). In contrast, IP-10 was increased more in subjects who went on to

4

98   become carriers (2.4-fold increase, p = 0.0008) than in those who remained carriage-negative (1.5-

99   fold increase, p = 0.051). Moreover, subjects with increased levels of IP-10 before inoculation

100   displayed higher pneumococcal density following Spn inoculation (Fig 1d). This suggests that

101   differences in the response to influenza virus are associated with secondary susceptibility to Spn.

102   To test whether this was specific for LAIV infection, we measured IP-10 in nasal washes from an

103   independent cohort in which a subset of subjects had asymptomatic viral upper respiratory tract

104   infection before Spn inoculation. These comprised rhinovirus (n=12), coronavirus (n=5), respiratory

105   syncytial virus (n=2) and parainfluenzavirus (n=1) [29]. The predominant virus, rhinovirus, was

106   recently shown to associate with increased pneumococcal acquisition and transmission [30]. In these

107   virus-infected subjects, levels of IP-10 were increased (Fig S2), and baseline IP-10 levels

108   correlated with increased pneumococcal density also in this second cohort (r = 0.32, p = 0.02, Fig

109   1e). While the correlation was modest in this validation cohort suggesting that other host and

110   environmental factors are involved, this is the first time a biomarker predicting Spn density has

111   been identified.

112   **Early neutrophil degranulation in response to carriage is impaired by LAIV infection**

113   In murine models, neutrophil recruitment after onset of carriage contributes to control of the

114   bacteria [15]. We observed pre-existent high levels of neutrophils in the human nose and

115   pneumococcal carriage did not lead to significant further recruitment of neutrophils (Fig S3a,b). To

116   investigate whether luminal neutrophils were involved in the early control of carriage, we measured

117   myeloperoxidase (MPO) levels, a marker for neutrophil degranulation [31], in nasal wash. Levels

118   were increased (2.2-fold, p < 0.05) at 2 days after challenge in control carriage+ but not carriage-

119   individuals (Fig 2a). This neutrophil activation was impaired in the LAIV group, who displayed high

120   carriage density during early carriage and had increased acquisition compared to controls.

121   Together, this suggests that neutrophil degranulation is important for the initial control of carriage.

122   To investigate whether neutrophils were also impaired systemically following LAIV as reported

123   during wild-type influenza infection [32], we isolated blood neutrophils before, and at three days after,

124   LAIV administration from a subset of subjects. We confirmed that opsonophagocytic killing of Spn

125   by blood neutrophils was decreased following LAIV (Fig 2b, p < 0.05). This effect could be

126   mimicked by the addition of TNF-α, but not IP-10, to neutrophils from healthy donors *in vitro,*

127   decreasing killing capacity in a dose-dependent manner (Fig 2c,d). Nanostring expression analysis

128   of 594 genes revealed 10 differentially expressed genes in blood neutrophils 3 days post LAIV

129   (Table S2). Among those were *MAP4K2* (3.2-fold increase, p=3.2x10^{-5}), which acts on the TNF-α

130   signal transduction pathway [33], and *TIGIT* (3.6-fold increase, p=0.008, Fig 2e). *TIGIT* expression

131   levels also negatively correlated with neutrophil killing capacity (r=-0.73, p=0.02, Fig 2f). TIGIT is

132   an "immune checkpoint" protein, which has been described to promote Treg cell function [34], but its

133   expression on neutrophils has not been previously appreciated. Incubation of whole blood with

134   recombinant TNF-α increased TIGIT levels on neutrophil surface within 30 minutes in a dose-

135   dependent manner (Fig 2g).

136   **Pneumococcal carriage-induced monocytes recruitment to the nose is impaired by LAIV**

137   **infection**

138   Immunophenotyping revealed a significant recruitment of monocytes to the nose following

139   establishment of carriage (Fig 3a,b and Fig S4). Monocyte levels increased as early as 2 days

140   following Spn inoculation, peaked at 9 days (median 4.8x increase) and remained elevated 29

141   days post Spn inoculation. In contrast, there was no recruitment of CD3+ T cells to the nose (Fig

142   S4b). LAIV infection prior to pneumococcal carriage impaired the recruitment of monocytes to the

143   nose (Fig 3a,b). Moreover, peak pneumococcal density associated with increased monocyte

144   recruitment in the control group (r=0.51, p=0.02), but not the LAIV group (r=0.08, p=0.70; Fig 3c,d).

145   Indeed, for subjects in the control group with very low carriage densities, which were only

146   detectable by molecular methods, no monocyte recruitment was observed (Fig S4c). This suggests

147   that a minimum Spn load is required for sensing and monocyte recruitment and that LAIV infection

148   interferes with this process. While MCP-1 was not significantly induced following Spn carriage,

149   levels correlated with numbers of monocytes at all timepoints (Fig S5a). Furthermore, stratification

6

150 of individuals showed that those with increased MCP-1 levels at day 2 post Spn inoculation exhibit

151 increased monocyte recruitment (Fig S5b). Levels of IL-6, IFN-γ and TNF-α also correlated with

152 levels of monocytes at each time point, but stratification of individuals did not reveal a differential

153 recruitment of monocytes (Fig S5a,b). In a second, independent cohort that did not receive any

154 vaccine, monocytes were increased at day 9 following Spn inoculation, which correlated with

155 increased MCP-1 levels in nasal fluid, validating these results (Table S3 and Fig S5c).

156 **Nasal responses associated with pneumococcal clearance are impaired by LAIV**

157 To assess anti-pneumococcal responses induced by carriage, we collected nasal cells 29 days

158 post Spn inoculation and stimulated *in vitro* with heat-killed Spn and measured levels of 30

159 cytokines in supernatant. An increased production (FC > 2 and q < 0.05 to unstimulated control) of

160 TNF-α, MIP-1α, IL-10, IL-6 and GM-CSF upon restimulation was observed in the control carriage+

161 group (Fig 4a and Fig S6a). In the LAIV carriage+ group, however, this boosting of anti-

162 pneumococcal cytokine responses by re-challenge was absent (Fig 4a and Fig S6a). The

163 production of the above five cytokines correlated with decreased density at day 29 post Spn

164 inoculation, suggesting these responses are involved in Spn clearance (Fig 4b). To test whether

165 monocytes/macrophages were the source of these cytokines we compared the cytokine signature

166 from whole nasal cells with that from alveolar macrophages exposed to Spn *in vitro* (Fig 4c).

167 Relative cytokine production highly correlated (r = 0.66, p < 0.0001) between the two cell

168 populations, suggesting that nasal monocytes/macrophages could be the source of these

169 cytokines. This is supported by the observation that in carriers with low carriage density (only

170 detectable by molecular methods), absence of monocyte recruitment associated with absent Spn-

171 specific responses (Fig S6b)

172 **LAIV alters nasal gene expression responses to carriage**

173 To identify gene signatures associated with the observed responses to pneumococcal carriage and

174 infection with LAIV, we performed RNA-sequencing on whole nasal cells at days -5, 2 and 9 from

175 Spn inoculation (Fig 5 and Table S4). Carriage without LAIV induced 834 and 176 differentially

7

176 expressed genes (DEG) at day 2 and day 9, respectively (Fig 5a). These genes were enriched for

177 pathways associated with Gap junction trafficking and regulation (including *GJA1*, *TJP1* and

178 multiple *GJB*) and degradation of the extracellular matrix (including *COL17A1*, *COL12A1*, *LAMA3*,

179 *KLK7*). In the carriage- group, a smaller number of DEG was observed (161 and 248 at day 2 and

180 day 9, respectively).

181 In the LAIV carriage+ group, 936 and 711 DEG were observed at day 2 and day 9, respectively.

182 Surprisingly, despite the high levels of inflammatory cytokines observed in the LAIV carriage-

183 group, only a relatively small number of DEG were observed at days 2 and 9 (126 and 153,

184 respectively). DEG of carriage+ subjects receiving LAIV and DEG of carriage+ without LAIV

185 showed very little overlap with only 38 DEG at day 2 and 2 DEG at day 9 in common. Very little

186 overlap was also observed on the pathway level between these groups, indicating LAIV alters the

187 natural responses to pneumococcus (Fig 5b and Table S5). This could reflect transcriptome

188 kinetics, such as observed in altered differentiation and cellular activation, or changes in cell

189 migration to the nasal mucosa.

190 The LAIV carriage+ group showed an enrichment for genes in TLR3 signalling cascade, RIG-

191 I/MDA5 mediated induction of IFN-alpha/beta pathways and IFN-gamma signalling, which is in

192 agreements with the induction of antiviral responses following LAIV vaccination [35]. Moreover, TLR4

193 signalling was also enriched in this group. The pneumococcal protein pneumolysin is sensed by

194 TLR4 [36] and it is possible that the increased pneumococcal density following LAIV vaccination led

195 to increased pneumolysin sensing. O-linked glycosylation of mucins, which are used by Spn as a

196 carbohydrate source for growth [37], was also enriched in the LAIV carriage+ group (including genes

197 *ST3GAL4*, *GALNT7*, *GCNT3*, *B4GALT5*). *ST3GAL4* is a sialyl transferase and cleavage of sialic

198 acids by the influenza neuraminidase has previously been shown to promote pneumococcal

199 growth [38]. This finding supports a LAIV-mediated effect on pneumococcal growth through

200 alterations of host factors. Common genes and pathways between the LAIV-vaccinated and control

8

201 carriers include "Innate immune system" and "Signaling by interleukins" (*IL1B*, *CLEC4E*, *CD55*,

202 *IL1RN*).

203

Gene modules associated with recruitment of monocytes

205 To identify sets of co-expressed genes post LAIV and carriage, we ran our program CEMiTool on

206 the baseline-normalized data of LAIV and control groups, separately [39]. This modular expression

207 analysis revealed the genes that may act together or are similarly regulated during the immune

208 responses to carriage/infection.

209 Genes in the control cohort were grouped into four co-expression modules, of which three were

210 significantly enriched for known Reactome pathways (Supp html file 1). Module M1 was enriched

211 in carriage+ at day 9 post Spn inoculation (Fig 6a). Levels of monocytes correlated with the

212 average fold change count in this module, suggesting that these genes reflect the infiltration of

213 monocytes (r = 0.61, p = 0.03, Fig 6b). To further investigate these monocytes, we performed gene

214 set enrichment analysis on the Module M1 genes using list of genes from distinct monocyte

215 subsets (Fig 6c) [40]. These genes were enriched for classical CD14+CD16- monocytes (p =

216 0.00002) and not for other monocyte subsets. Moreover, this module was enriched for genes

217 related to "chemokine receptors bind chemokines" and "interferon α/β signalling" (Fig 6d). Type I

218 interferon has been shown to be required for the clearance of pneumococcal carriage in murine

219 models [41] and these findings suggest that their activity in monocytes might be critical for this.

220 CEMiTool also integrates co-expression analysis with protein-protein interaction data. Expression

221 of *CXCL6* and its receptor *CXCR2* were identified as hubs in this module M1 (Fig 6e and Supp

222 html file 1). CXCR2 engagement has been shown to induce attachment of monocytes to the

223 endothelial layer, initiating chemotaxis, which suggests this interaction could contribute to

224 monocyte recruitment [42]. Module M3 was enriched in genes related to "extracellular matrix

225 organization" and "collagen formation" (Fig S7).

9

226   For LAIV, we identified six distinct co-expression modules (Supp html file 2), which were strongly

227   enriched in genes related to "Diseases associated with O-glycosylation of proteins" (module M1),

228   "Immunoregulatory interactions between a lymphoid and a non-Lymphoid cell" (module M3),

229   "chemokine receptors bind chemokines" (module M4), as well as "interferon signalling" (module

230   M5, Fig S8). Indeed, the hubs of module M5 are well known type I interferon-related genes, such

231   as *ISG15*, *OAS1*, *OASL*, *IFIT1-3*, and *IFITM1*. Altogether, our findings reveal that a strong local

232   antiviral response is elicited in response to LAIV infection.

233   **Discussion**

234   This study addresses fundamental questions about the immune responses that control and clear

235   Spn carriage and how influenza infection can alter this control. By using for the first time a double

236   experimental human challenge model with LAIV and Spn, we revealed that Spn carriage led to a

237   quick degranulation of pre-existent nasal neutrophils in the human nose and recruitment of

238   monocytes, promoting bacterial clearance. LAIV infection impaired these immune responses

239   following carriage. LAIV is an attenuated influenza strain and wild-type influenza viruses might

240   have even more pronounced effects on the host response to pneumococcus. Carriage in the

241   absence of LAIV was associated with only limited inflammation, corroborating the view of Spn as a

242   commensal bacterium that can asymptomatically colonize healthy adults [43]. In contrast, robust pro-

243   inflammatory cytokine responses were measured following LAIV at both the protein and gene

244   expression level. Altogether, these results provide explanation for our previous report that LAIV

245   increased acquisition of Spn and carriage density [14].

246   In addition, our findings that LAIV led to impaired blood neutrophil killing capacity and that the

247   addition of TNF-α, which was increased following LAIV, to neutrophils *in vitro* impaired their

248   activity, highlights their crucial roles in susceptibility to secondary bacterial infection [44]. The

249   association of TIGIT in this impaired neutrophil function following influenza infection warrants

250   further investigation as TIGIT-blocking therapeutics are currently being developed for cancer and

251   HIV treatment [45].

252 We identified IP-10 as a marker for increased susceptibility to Spn and propose this should be

253 further investigated as a potential therapeutic target for secondary bacterial infections associated

254 with virus infections. Our data showed that individuals with higher levels of IP-10 prior to Spn

255 inoculation had higher bacterial density. In a recent study, children with pneumonia with viral and

256 bacterial (predominantly pneumococcal) co-infection had increased levels of IP-10 compared to

257 children with just viral or bacterial pneumonia, which associated with disease severity [46]. Murine

258 data suggests that IP-10 plays a direct role during pneumonia. Mice with genetic ablation of

259 CXCR3, the receptor for IP-10, CXCL9 and CXCL11, showed increased survival, decreased lung

260 inflammation and less invasion following infection, depending on pneumococcal inoculation strain

261 used [47]. Moreover, addition of exogenous IP-10 prior to infection of mice with influenza or RSV

262 increased pneumonia severity [48].

263 Our results support previous findings from murine models showing that MCP-1 signalling and

264 monocyte recruitment are key mediators of pneumococcal carriage clearance [16]. However,

265 contrary to key mechanisms described in murine models, we did not observe any production of IL-

266 17A or neutrophil recruitment to the nose following carriage or associated with carriage clearance

267 [15-17], underlining the importance of confirmation of murine findings by human data.

268 One limitation of this study is that only one pneumococcal serotype 6B isolate was used, future

269 studies using other isolates with a more or less invasive phenotype will be able to answer how

270 generalizable these findings across pneumococcal isolates are. Nonetheless, the observation that

271 carriage density and duration declines in parallel for all serotypes following repeated exposure,

272 suggests that immunological control of newly-acquired Spn is mediated by similar mechanisms

273 independent of the colonizing serotype [49].

274 In conclusion, this study highlighted the importance for innate immunity in the control of carriage

275 density and clearance of Spn, which was impaired by pre-existing viral infections (Fig S9).

276 Secondary bacterial infection following viral respiratory tract infection has a large burden of

11

277 disease worldwide and disrupting viral-bacterial synergy through host-directed therapy could prove

278 an attractive addition to current therapeutic and vaccination options [50].

279 **Methods**

280 **Study design and sample collection**

281 Healthy adult volunteers were 1:1 randomized to receive either intranasally LAIV (2015/2016

282 Fluenz Tetra or FluMist Tetra, AstraZeneca, UK) or intramuscular Quadrivalent Inactivated

283 Influenza Vaccination (Fluarix Tetra, GlaxoSmithKline, UK) as described previously [14]. The control

284 group also received a nasal saline spray, while the LAIV group also received a intramuscular

285 saline injection. Three days post vaccination all subjects were inoculated with 80,000 CFU per

286 nostril of 6B type Spn as described [6,51]. Nasal microbiopsies (ASL Rhino-Pro[©], Arlington Scientific)

287 and nasal lining fluid (Nasosorption™, Hunt Developments) samples were collected and stored at -

288 80C as previously described [52].

289 **Clinical Trial details**

290 The double-blinded randomized clinical LAIV-EHPC trial was registered on EudraCT (Number

291 2014-004634-26) on 28th April 2015 and ISRCTN (Number 16993271) on 2nd Sep 2015 and was

292 co-sponsored by the Royal Liverpool University Hospital and the Liverpool School of Tropical

293 Medicine. Key eligibility criteria included: capacity to give informed consent, no

294 immunocompromised state or contact with susceptible individuals, no influenza vaccine or infection

295 in the last two years and not having taken part in EHPC studies in the past three years. The

296 primary endpoint was the occurrence of pneumococcal colonisation determined by the presence of

297 pneumococcus in nasal wash samples (NW) at any time point post inoculation up to and including

298 day 29, detected using classical microbiology or *lytA* qPCR as described [6,51,53]. In this study, 130

299 volunteers were inoculated with pneumococcus, giving an 80% power to identify a 50% increase in

300 carriage acquisition. Of 130 vaccinated volunteers, five were natural pneumococcal carriers (two in

301 LAIV arm and three in control arm) and were excluded from further analysis. Another 8 subjects in

12

302   the LAIV arm were excluded following a systematic LAIV dispensing error by a single practitioner,

303   as recommended by the trial steering group. This resulted in a final 55 subjects analysed in the

304   LAIV arm and 62 subjects in the control arm. Key secondary endpoints included the density of

305   pneumococcal colonisation in NW at each time point following pneumococcal inoculation (days 2,

306   7, 9, 14, 22 and 29), detected using classical microbiology, the area under the curve of

307   pneumococcal colonisation density following pneumococcal inoculation (days 2, 7, 9, 14 , 22 and

308   29), detected using classical microbiology or by molecular methods (*lytA*), and the immunological

309   mechanisms associated with altered susceptibility to pneumococcus following LAIV. The outcomes

310   reported in this manuscript were a priori included in the study protocol.

311   **Ethics statement**

312   All volunteers gave written informed consent and research was conducted in compliance with all

313   relevant ethical regulations. Ethical approval was given by the East Liverpool NHS Research and

314   Ethics Committee (REC)/Liverpool School of Tropical Medicine (LSTM) REC, reference numbers:

315   15/NW/0146 and 14/NW/1460 and Human Tissue Authority licensing number 12548.

316   **Flow cytometry analysis**

317   Immunophenotyping of nasal cells obtained by curettes was performed as described [52]. In brief,

318   cells were dislodged from curettes and stained with LIVE/DEAD® Fixable Aqua Dead Cell Stain

319   (ThermoFisher) and an antibody cocktail containing Epcam-PE, HLADR-PECy7, CD16-APC,

320   CD66b-FITC (all Biolegend), CD3-APCCy7, CD14-PercpCy5.5 (BD Biosciences) and CD45-

321   PACOrange (ThermoFisher). Whole blood was stained for 15 min at room temperature with TIGIT-

322   PECy7 (Biolegend) and CD16-APC, followed by 2x 10 min incubation steps with FACSLysis buffer

323   (BD Biosciences) to remove erythrocytes. Samples were acquired on a LSRII flow cytometer (BD)

324   and analysed using Flowjo X (Treestar). Fluorescent minus one controls for each of the included

325   antibodies were used to validate results. For the LAIV and control cohorts, but not the additional

326   validation cohort (Fig S5C), 84/553 samples (15.2%) with less than 500 immune cells or 250

327   epithelial cells were excluded from further analysis.

13

328   **Neutrophil opsonophagocytic killing**

329   Neutrophil killing capacity was evaluated as previously described with minor modifications [54].

330   Briefly, neutrophils were isolated through density gradient centrifugation, followed by 45 min

331   incubation with serotype 6B pneumococci (inoculation strain, MOI 100:1), baby rabbit complement

332   (Mast Group, Bootle, UK) and human intravenous immunoglobulin (IVIG; Gamunex, Grifols Inc,

333   Spain). In some experiments, recombinant TNF-α or IP-10 (Biotechne) was added.

334   **Luminex analysis of nasal lining fluid or stimulated nasal cells**

335   Nasal cells collected in RPMI containing 1% penicillin/streptomycin/neomycin (ThermoFisher) and

336   10% heat-inactivated FBS (ThermoFisher) were incubated with 50ug/mL DNAse I (Sigma Aldrich)

337   at room temperature for 20 min and filtered over a 70um filter (ThermoFisher). Cells were spun

338   down at 440xg for 5 min, resuspended, counted and incubated at 250,000 cells/mL in 96-wells or

339   384-wells plates (ThermoFisher). Heat-killed Spn inoculation strain was added at a concentration

340   of 5 ng/mL of total protein (corresponding to 4.3x10^7 CFU/mL) and cells were incubated for 18 h.

341   Bacterial protein concentration was measured by Bradford assay, using bovine serum albumin as

342   standard and titration experiments were performed to determine dose. Supernatant was collected

343   and stored at -80C until analysis. For nasosorption filters, cytokines were eluted from stored filters

344   using 100 uL of assay buffer (ThermoFisher) by centrifugation, then the eluate was cleared by

345   further centrifugation at 16,000g. Prior to analysis, samples were centrifuged for 10 min at

346   16,000xg to clear samples. These were acquired on a LX200 using a 30-plex magnetic human

347   Luminex cytokine kit (ThermoFisher) and analysed with xPonent3.1 software following

348   manufacturer's instructions. Samples were analysed in duplicates and nasosorption samples with

349   a CV > 25% were excluded.

350   **RNA extraction and sequencing**

351   Nasal cells were collected in RNALater (ThermoFisher) at -80C until extraction. Extraction was

352   performed using the RNEasy micro kit (Qiagen) with on column DNA digestion. Extracted RNA

14

353   was quantified using a Qubit™ (ThermoFisher). Sample integrity assessment (Bioanalyzer,

354   Agilent), library preparation and RNA-sequencing (Illumina Hiseq4000, 20M reads, 100 paired-end

355   reads) were performed at the Beijing Genome Institute (China).

356   **Nanostring**

357   Purified blood neutrophils were stored in RLT buffer (Qiagen) with 1% 2-mercaptoethanol (Sigma)

358   at -80C until RNA extraction as above. The single cell immunology v2 kit (Nanostring) was used

359   with 20 pre-amp cycles for all samples. Hybridized samples were prepared on a Prep Station and

360   scanned on a nCounter® MAX (Nanostring). Raw counts were analysed using DESeq2 using

361   internal normalization, which gave lower variance than normalizing to included housekeeping

362   genes. DEG were identified using a model matrix correcting for repeated individual measurements.

363   Log counts per million (CPM) from raw counts were calculated using the 'edgeR' package.

364   **RNA sequencing analysis**

365   Quality control of raw sequencing data was done using fastQC. Mapping to a human reference

366   genome assembly (GRCh38) was done using STAR 2.5.0a [55]. Read counts from the resulting

367   BAM alignment files were obtained with featureCounts using a GTF gene annotation from the

368   Ensembl database [56,57]. The R/Bioconductor package DESeq2 was used to identify differentially

369   expressed genes among the samples, after removing absent features (zero counts in more than

370   75% of samples) [58]. Genes with an FDR value < 0.1 and an absolute fold change (FC) > 1.5 were

371   identified as differentially expressed.

372   **Co-expression analysis**

373   For co-expression analysis, counts were normalized using log CPM and the log2 fold change was

374   calculated for each time point in a subject-wise manner. The co-expression analysis was

375   performed separately for each group (control and LAIV) using the CEMiTool package developed

376   by   our   group   and   available   at   Bioconductor

15

377 (https://bioconductor.org/packages/release/bioc/html/CEMiTool.html) [39]. This package unifies the

378 discovery and the analysis of coexpression gene modules, evaluating if modules contain genes

379 that are over-represented by specific pathways or that are altered in a specific sample group. A p-

380 value = 0.05 was applied for filtering lowly expressed genes

Statistical analysis

382 All experiments were performed randomised and blinded. Two-tailed statistical tests are used

383 throughout the study. When log-normalized data was not normally distributed, non-parametric tests

384 were performed and multiple correction testing (Benjamin-Hochberg) was applied for gene

385 expression and Luminex analysis.

386

Data availability

388 Raw RNA-sequencing data have been deposited in the GEO repository. All other underlying data

389 is provided in the manuscript

Acknowledgements

Author contributions

16

401 SPJ contributed to conceiving, designing, performing and analysing experiments and writing of the

402 paper. FM and HIN contributed analysing experiments and writing of the paper. BFC, MH, EM, ES,

403 JFG, CS, JR, SP, EN, ELG, WAASP, DB contributed to conducting and analysing experiments.

404 AHW, HH, CH, HA, SZ, VC, JR contributed to sample collection and design of the study. DMF

405 contributed to conceiving, designing and analysing experiments, design of the study and writing of

406 the paper. All authors have read and approved the manuscript.

409 **References**

410 1 Liu, L. *et al.* Global, regional, and national causes of under-5 mortality in 2000-15: an
411 updated systematic analysis with implications for the Sustainable Development Goals.
412 *Lancet* **388**, 3027-3035, doi:10.1016/S0140-6736(16)31593-8 (2016).
413 2 Morens, D. M., Taubenberger, J. K. & Fauci, A. S. Predominant role of bacterial pneumonia
414 as a cause of death in pandemic influenza: implications for pandemic influenza
415 preparedness. *J Infect Dis* **198**, 962-970, doi:10.1086/591708 (2008).
416 3 Goldblatt, D. *et al.* Antibody Responses to Nasopharyngeal Carriage of Streptococcus
417 pneumoniae in Adults: A Longitudinal Household Study. *Journal of Infectious Diseases*
418 **192**, 387-393 (2005).
419 4 Simell, B. *et al.* The fundamental link between pneumococcal carriage and disease. *Expert*
420 *review of vaccines* **11**, 841-855, doi:10.1586/erv.12.53 (2012).
421 5 Melegaro, A., Gay, N. J. & Medley, G. F. Estimating the transmission parameters of
422 pneumococcal carriage in households. *Epidemiol Infect* **132**, 433-441 (2004).
423 6 Ferreira, D. M. *et al.* Controlled human infection and rechallenge with Streptococcus
424 pneumoniae reveals the protective efficacy of carriage in healthy adults. *Am J Respir Crit*
425 *Care Med* **187**, 855-864, doi:10.1164/rccm.201212-2277OC (2013).
426 7 McCool, T. L., Cate, T. R., Moy, G. & Weiser, J. N. The immune response to pneumococcal
427 proteins during experimental human carriage. *J.Exp.Med.* **195**, 359 (2002).
428 8 Mina, M. J. & Klugman, K. P. The role of influenza in the severity and transmission of
429 respiratory bacterial disease. *Lancet Respir Med* **2**, 750-763, doi:10.1016/S2213-
430 2600(14)70131-6 (2014).
431 9 Alpkvist, H. *et al.* Clinical and Microbiological Factors Associated with High
432 Nasopharyngeal Pneumococcal Density in Patients with Pneumococcal Pneumonia. *PLoS*
433 *One* **10**, e0140112, doi:10.1371/journal.pone.0140112 (2015).
434 10 Wolter, N. *et al.* High nasopharyngeal pneumococcal density, increased by viral coinfection,
435 is associated with invasive pneumococcal pneumonia. *J Infect Dis* **210**, 1649-1657,
436 doi:jiu326 [pii]

437 10.1093/infdis/jiu326.

17

438 11 Albrich, W. C. *et al.* Pneumococcal colonisation density: a new marker for disease severity
439   in HIV-infected adults with pneumonia. *BMJ Open* **4**, e005953, doi:10.1136/bmjopen-2014-
440   005953 (2014).
441 12 Thors, V. *et al.* The Effects of Live Attenuated Influenza Vaccine on Nasopharyngeal
442   Bacteria in Healthy 2 to 4 Year Olds. A Randomized Controlled Trial. *Am J Respir Crit*
443   *Care Med* **193**, 1401-1409, doi:10.1164/rccm.201510-2000OC (2016).
444 13 Mina, M. J., McCullers, J. A. & Klugman, K. P. Live attenuated influenza vaccine enhances
445   colonization of Streptococcus pneumoniae and Staphylococcus aureus in mice. *mBio* **5**,
446   doi:mBio.01040-13 [pii]

447 10.1128/mBio.01040-13.
448 14 Rylance, J. *et al.* Effect of Live Attenuated Influenza Vaccine on Pneumococcal Carriage.
449   *bioRxiv*, doi:10.1101/343319 (2018).
450 15 Lu, Y. J. *et al.* Interleukin-17A mediates acquired immunity to pneumococcal colonization.
451   *PLoS Pathog* **4**, e1000159, doi:10.1371/journal.ppat.1000159 (2008).
452 16 Zhang, Z., Clarke, T. B. & Weiser, J. N. Cellular effectors mediating Th17-dependent
453   clearance of pneumococcal colonization in mice. *J Clin Invest* **119**, 1899-1909,
454   doi:10.1172/JCI36731 (2009).
455 17 Lu, Y. J. *et al.* GMP-grade pneumococcal whole-cell vaccine injected subcutaneously
456   protects mice from nasopharyngeal colonization and fatal aspiration-sepsis. *Vaccine* **28**,
457   7468-7475, doi:10.1016/j.vaccine.2010.09.031 (2010).
458 18 Nakamura, S., Davis, K. M. & Weiser, J. N. Synergistic stimulation of type I interferons
459   during influenza virus coinfection promotes Streptococcus pneumoniae colonization in
460   mice. *J Clin Invest* **121**, 3657-3665, doi:10.1172/JCI57762 (2011).
461 19 Sun, K. & Metzger, D. W. Inhibition of pulmonary antibacterial defense by interferon-
462   gamma during recovery from influenza infection. *Nat Med* **14**, 558-564, doi:nm1765 [pii]

463 10.1038/nm1765 (2008).
464 20 Li, W., Moltedo, B. & Moran, T. M. Type I interferon induction during influenza virus
465   infection increases susceptibility to secondary Streptococcus pneumoniae infection by
466   negative regulation of gammadelta T cells. *J Virol* **86**, 12304-12312,
467   doi:10.1128/JVI.01269-12 (2012).
468 21 Jochems, S. P., Weiser, J. N., Malley, R. & Ferreira, D. M. The immunological mechanisms
469   that control pneumococcal carriage. *PLoS Pathog* **13**, e1006665,
470   doi:10.1371/journal.ppat.1006665 (2017).
471 22 Querec, T. D. *et al.* Systems biology approach predicts immunogenicity of the yellow fever
472   vaccine in humans. *Nat Immunol* **10**, 116-125, doi:10.1038/ni.1688 (2009).
473 23 Oh, J. Z. *et al.* TLR5-mediated sensing of gut microbiota is necessary for antibody
474   responses to seasonal influenza vaccination. *Immunity* **41**, 478-492,
475   doi:10.1016/j.immuni.2014.08.009 (2014).
476 24 Li, S. *et al.* Metabolic Phenotypes of Response to Vaccination in Humans. *Cell* **169**, 862-
477   877 e817, doi:10.1016/j.cell.2017.04.026 (2017).
478 25 Kazmin, D. *et al.* Systems analysis of protective immune responses to RTS,S malaria
479   vaccination in humans. *Proceedings of the National Academy of Sciences of the United*
480   *States of America* **114**, 2425-2430, doi:10.1073/pnas.1621489114 (2017).
481 26 Nakaya, H. I. *et al.* Systems biology of vaccination for seasonal influenza in humans. *Nat*
482   *Immunol* **12**, 786-795, doi:10.1038/ni.2067 (2011).

483   27   Nakaya, H. I. *et al.* Systems Analysis of Immunity to Influenza Vaccination across Multiple
484   Years and in Diverse Populations Reveals Shared Molecular Signatures. *Immunity* **43**, 1186-
485   1198, doi:10.1016/j.immuni.2015.11.012 (2015).
486   28   Li, S. *et al.* Molecular signatures of antibody responses derived from a systems biology
487   study of five human vaccines. *Nat Immunol* **15**, 195-204, doi:10.1038/ni.2789 (2014).
488   29   Glennie, S. *et al.* Modulation of nasopharyngeal innate defenses by viral coinfection
489   predisposes individuals to experimental pneumococcal carriage. *Mucosal Immunol*,
490   doi:10.1038/mi.2015.35 (2015).
491   30   Karppinen, S. *et al.* Acquisition and Transmission of Streptococcus pneumoniae Are
492   Facilitated during Rhinovirus Infection in Families with Children. *Am J Respir Crit Care*
493   *Med* **196**, 1172-1180, doi:10.1164/rccm.201702-0357OC (2017).
494   31   Segal, A. W. How neutrophils kill microbes. *Annu Rev Immunol* **23**, 197-223,
495   doi:10.1146/annurev.immunol.23.021704.115653 (2005).
496   32   Craft, A. W., Reid, M. M. & Low, W. T. Effect of virus infections on polymorph function in
497   children. *Br Med J* **1**, 1570 (1976).
498   33   Yuasa, T., Ohno, S., Kehrl, J. H. & Kyriakis, J. M. Tumor necrosis factor signaling to stress-
499   activated protein kinase (SAPK)/Jun NH2-terminal kinase (JNK) and p38. Germinal center
500   kinase couples TRAF2 to mitogen-activated protein kinase/ERK kinase kinase 1 and SAPK
501   while receptor interacting protein associates with a mitogen-activated protein kinase kinase
502   kinase upstream of MKK6 and p38. *J Biol Chem* **273**, 22681-22692 (1998).
503   34   Anderson, A. C., Joller, N. & Kuchroo, V. K. Lag-3, Tim-3, and TIGIT: Co-inhibitory
504   Receptors with Specialized Functions in Immune Regulation. *Immunity* **44**, 989-1004,
505   doi:10.1016/j.immuni.2016.05.001 (2016).
506   35   Wu, W. *et al.* RIG-I and TLR3 are both required for maximum interferon induction by
507   influenza virus in human lung alveolar epithelial cells. *Virology* **482**, 181-188,
508   doi:10.1016/j.virol.2015.03.048 (2015).
509   36   Malley, R. *et al.* Recognition of pneumolysin by Toll-like receptor 4 confers resistance to
510   pneumococcal infection. *Proceedings of the National Academy of Sciences of the United*
511   *States of America* **100**, 1966-1971, doi:10.1073/pnas.0435928100 (2003).
512   37   Paixao, L. *et al.* Host glycan sugar-specific pathways in Streptococcus pneumoniae:
513   galactose as a key sugar in colonisation and infection [corrected]. *PLoS One* **10**, e0121042,
514   doi:10.1371/journal.pone.0121042 (2015).
515   38   Siegel, S. J., Roche, A. M. & Weiser, J. N. Influenza promotes pneumococcal growth during
516   coinfection by providing host sialylated substrates as a nutrient source. *Cell Host Microbe*
517   **16**, 55-67, doi:10.1016/j.chom.2014.06.005 (2014).
518   39   Russo, P. S. T. *et al.* CEMiTool: a Bioconductor package for performing comprehensive
519   modular co-expression analyses. *BMC Bioinformatics* **19**, 56, doi:10.1186/s12859-018-
520   2053-1 (2018).
521   40   Kwissa, M. *et al.* Dengue virus infection induces expansion of a CD14(+)CD16(+)
522   monocyte population that stimulates plasmablast differentiation. *Cell Host Microbe* **16**, 115-
523   127, doi:10.1016/j.chom.2014.06.001 (2014).
524   41   Parker, D. *et al.* Streptococcus pneumoniae DNA initiates type I interferon signaling in the
525   respiratory tract. *mBio* **2**, e00016-00011, doi:10.1128/mBio.00016-11 (2011).
526   42   Gerszten, R. E. *et al.* MCP-1 and IL-8 trigger firm adhesion of monocytes to vascular
527   endothelium under flow conditions. *Nature* **398**, 718-723, doi:10.1038/19546 (1999).
528   43   Weiser, J. N. The pneumococcus: why a commensal misbehaves. *J Mol Med (Berl)* **88**, 97-
529   102, doi:10.1007/s00109-009-0557-x (2010).

530 44 Rynda-Apple, A., Robinson, K. M. & Alcorn, J. F. Influenza and Bacterial Superinfection:
531   Illuminating the Immunologic Mechanisms of Disease. *Infect Immun* **83**, 3764-3770,
532   doi:10.1128/IAI.00298-15 (2015).
533 45 Cox, M. A., Nechanitzky, R. & Mak, T. W. Check point inhibitors as therapies for
534   infectious diseases. *Curr Opin Immunol* **48**, 61-67, doi:10.1016/j.coi.2017.07.016 (2017).
535 46 Hoffmann, J. *et al.* Viral and bacterial co-infection in severe pneumonia triggers innate
536   immune responses and specifically enhances IP-10: a translational study. *Sci Rep* **6**, 38532,
537   doi:10.1038/srep38532 (2016).
538 47 Seyoum, B., Yano, M. & Pirofski, L. A. The innate immune response to Streptococcus
539   pneumoniae in the lung depends on serotype and host response. *Vaccine* **29**, 8002-8011,
540   doi:10.1016/j.vaccine.2011.08.064 (2011).
541 48 Luo, H., Wang, D., Che, H. L., Zhao, Y. & Jin, H. Pathological observations of lung
542   inflammation after administration of IP-10 in influenza virus- and respiratory syncytial
543   virus-infected mice. *Exp Ther Med* **3**, 76-79, doi:10.3892/etm.2011.350 (2012).
544 49 Hogberg, L. *et al.* Age- and serogroup-related differences in observed durations of
545   nasopharyngeal carriage of penicillin-resistant pneumococci. *J Clin Microbiol* **45**, 948-952,
546   doi:10.1128/JCM.01913-06 (2007).
547 50 Madhi, S. A., Klugman, K. P. & Vaccine Trialist, G. A role for Streptococcus pneumoniae
548   in virus-associated pneumonia. *Nat Med* **10**, 811-813, doi:10.1038/nm1077 (2004).
549 51 Gritzfeld, J. F. *et al.* Experimental human pneumococcal carriage. *J Vis Exp*,
550   doi:10.3791/50115 (2013).
551 52 Jochems, S. P. *et al.* Novel Analysis of Immune Cells from Nasal Microbiopsy
552   Demonstrates Reliable, Reproducible Data for Immune Populations, and Superior Cytokine
553   Detection Compared to Nasal Wash. *PLoS One* **12**, e0169805,
554   doi:10.1371/journal.pone.0169805 (2017).
555 53 Gritzfeld, J. F. *et al.* Density and duration of experimental human pneumococcal carriage.
556   *Clin Microbiol Infect* **20**, O1145-1151, doi:10.1111/1469-0691.12752 (2014).
557 54 Morton, B. *et al.* Augmented Passive Immunotherapy with P4 Peptide Improves Phagocyte
558   Activity in Severe Sepsis. *Shock* **46**, 635-641, doi:10.1097/SHK.0000000000000715 (2016).
559 55 Dobin, A. *et al.* STAR: ultrafast universal RNA-seq aligner. *Bioinformatics* **29**, 15-21
560   (2013).
561 56 Liao, Y., Smyth, G. K. & Shi, W. featureCounts: an efficient general purpose program for
562   assigning sequence reads to genomic features. *Bioinformatics* **30**, 923-930 (2014).
563 57 Yates, A. *et al.* Ensembl 2016. *Nucleic Acids Res* **44**, D710-716, doi:10.1093/nar/gkv1157
564   (2016).
565 58 Love, M. I., Huber, W. & Anders, S. Moderated estimation of fold change and dispersion
566   for RNA-seq data with DESeq2. *Genome Biol* **15**, 550, doi:10.1186/s13059-014-0550-8
567   (2014).

568
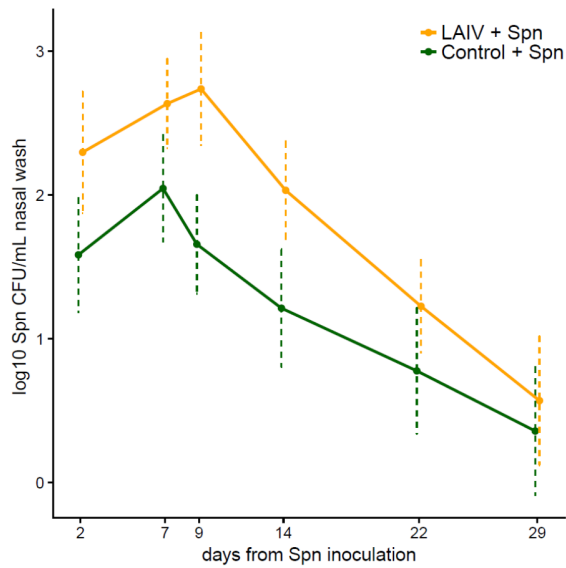
Supplementary Figure 1. Pneumococcal density in the LAIV and Control cohorts. Mean and standard error of log-transformed carriage density [CFU/mL nasal wash] for carriage-positive volunteers (defined by detection of Spn at any timepoint) are shown for the Spn group (green, n = 14-24 samples per time-point) and LAIV + Spn group (orange, n = 16-25). Density for samples with undetectable pneumococcal load was set at 0.1 CFU/mL nasal wash.
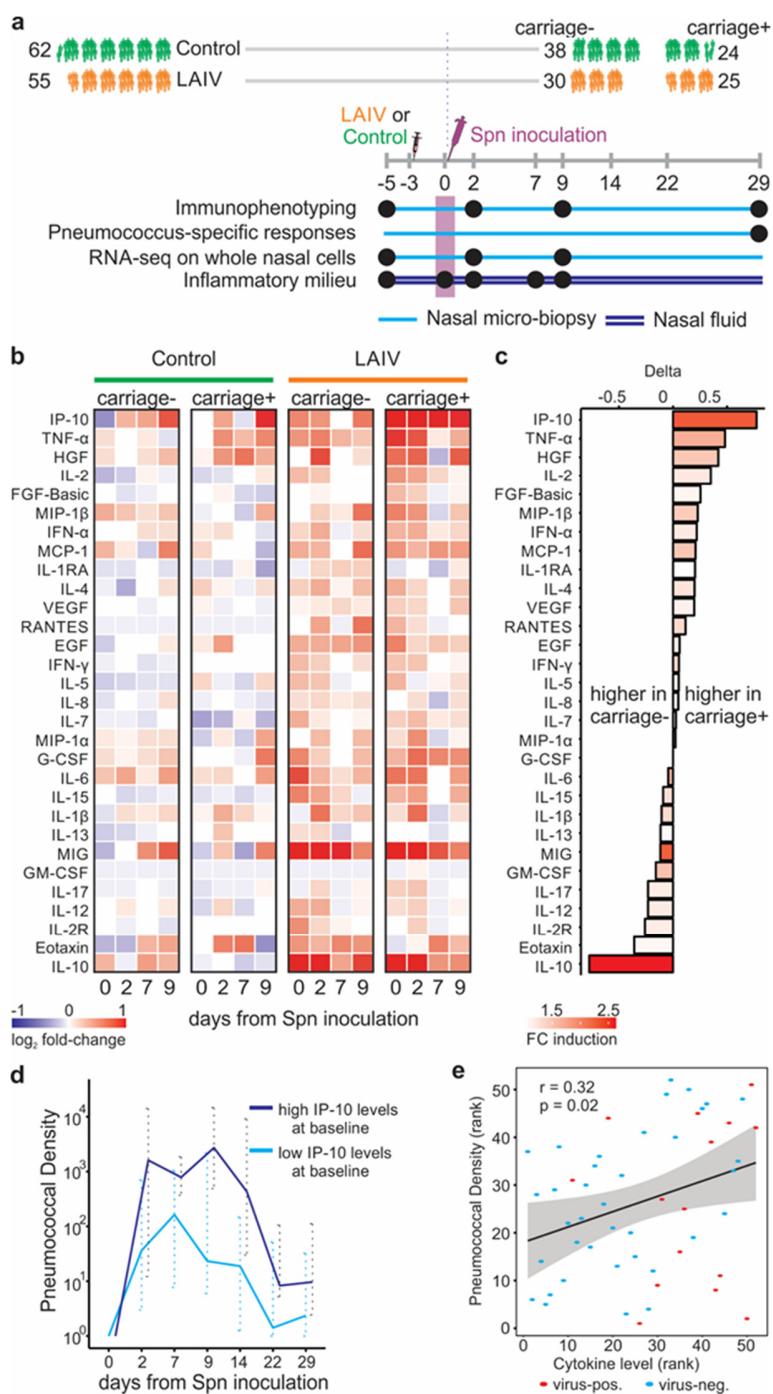
Figure 1. LAIV-pneumococcus co-infection leads to excessive pro-inflammatory responses that associate with increased pneumococcal density and impaired monocyte recruitment. a) Experimental design of the study. LAIV = live attenuated influenza vaccine, Spn = *Streptococcus pneumoniae*. Analysed timepoints are indicated by black circles. b) Heatmap showing for each cytokine the median log2 fold-change compared to baseline for the timepoints 0/2/7/9, n = 19 per group. c) The delta in median log fold change (FC) following LAIV vaccination just prior to inoculation with Spn for subjects becoming carriage+ or carriage- (excluding subjects becoming positive by PCR only, who resemble subjects that become carriage+ by

culture as well). The colour of each bar represents the median induction in the entire LAIV group. d) Pneumococcal density (median and interquartile range of CFU/mL nasal wash shown) for all carriage+ subjects with high (top quartile) or low (all subjects below top quartile) IP-10 levels at day 0. P = 0.019 by Mann-Whitney of AUC of log-transformed density over time. e) Scatter plot showing correlation of levels of IP-10 at baseline with Spn density for a second validation cohort (n = 52) with an asymptomatic upper respiratory tract virus infection (n=15) or not. Spearman correlation test results are shown.

Cytokine	median FC LAIV	median FC TIV	p-value LAIV	p-value TIV	adjusted p-value LAIV	adjusted p-value TIV
MCP_1	1.37	1.17	1.74E-05	9.27E-02	2.61E-04	9.22E-01
IFN-g	1.21	1.00	1.30E-05	4.02E-01	2.61E-04	9.22E-01
IP_10	1.58	0.95	9.18E-05	6.65E-01	7.29E-04	9.22E-01
IL_2	1.27	0.94	9.72E-05	4.83E-01	7.29E-04	9.22E-01
MIG	2.17	0.94	1.41E-04	7.42E-01	8.46E-04	9.22E-01
G_CSF	1.31	1.09	1.74E-04	1.66E-01	8.70E-04	9.22E-01
IL_15	1.34	1.00	3.31E-04	6.88E-01	1.42E-03	9.22E-01
IL_6	1.52	1.20	5.92E-04	2.02E-01	2.22E-03	9.22E-01
IL_4	1.16	1.03	1.13E-03	7.88E-01	3.77E-03	9.22E-01
IL_10	2.30	1.08	1.61E-03	5.07E-01	4.83E-03	9.22E-01
IL_12	1.22	1.03	4.13E-03	7.66E-01	1.03E-02	9.22E-01
IFN-a	1.14	1.03	3.96E-03	3.73E-01	1.03E-02	9.22E-01
MIP_1b	1.43	1.11	8.34E-03	6.99E-01	1.68E-02	9.22E-01
IL_7	1.16	0.96	8.39E-03	3.08E-01	1.68E-02	9.22E-01
IL_2R	1.13	1.03	7.33E-03	6.68E-01	1.68E-02	9.22E-01
MIP_1a	1.12	0.98	9.62E-03	8.23E-01	1.80E-02	9.22E-01
FGF-Basic	1.10	1.03	1.20E-02	7.74E-01	2.11E-02	9.22E-01
VEGF	1.13	1.05	1.27E-02	7.54E-01	2.11E-02	9.22E-01
TNF-a	1.65	1.06	1.45E-02	4.32E-01	2.29E-02	9.22E-01
HGF	1.40	1.11	1.66E-02	6.06E-01	2.49E-02	9.22E-01
IL_1b	1.10	1.02	4.42E-02	9.76E-01	6.32E-02	9.76E-01
IL_17	1.15	1.00	4.64E-02	8.30E-01	6.32E-02	9.22E-01
IL_5	1.20	1.07	6.67E-02	3.67E-01	8.70E-02	9.22E-01
IL_13	1.09	1.00	9.08E-02	7.15E-01	1.14E-01	9.22E-01
EGF	1.30	1.06	9.57E-02	3.21E-01	1.15E-01	9.22E-01
IL_8	1.08	0.98	1.04E-01	5.28E-01	1.20E-01	9.22E-01

RANTES	1.00	1.00	1.49E-01	8.79E-01	1.66E-01	9.42E-01
GM_CSF	1.00	1.00	4.95E-01	3.80E-01	5.31E-01	9.22E-01
Eotaxin	1.12	1.00	7.39E-01	9.56E-01	7.64E-01	9.76E-01
IL-1RA	1.00	0.97	9.05E-01	8.70E-02	9.05E-01	9.22E-01

Table S1. Cytokine induction following LAIV or control vaccination, prior to Spn inoculation. Levels of 30 cytokines in nasal fluid were measured before and 3 days after vaccination, just prior to pneumococcal challenge. Median FC, Wilcoxon p-values, and FDR-corrected p-values are depicted. N = 38 per group.
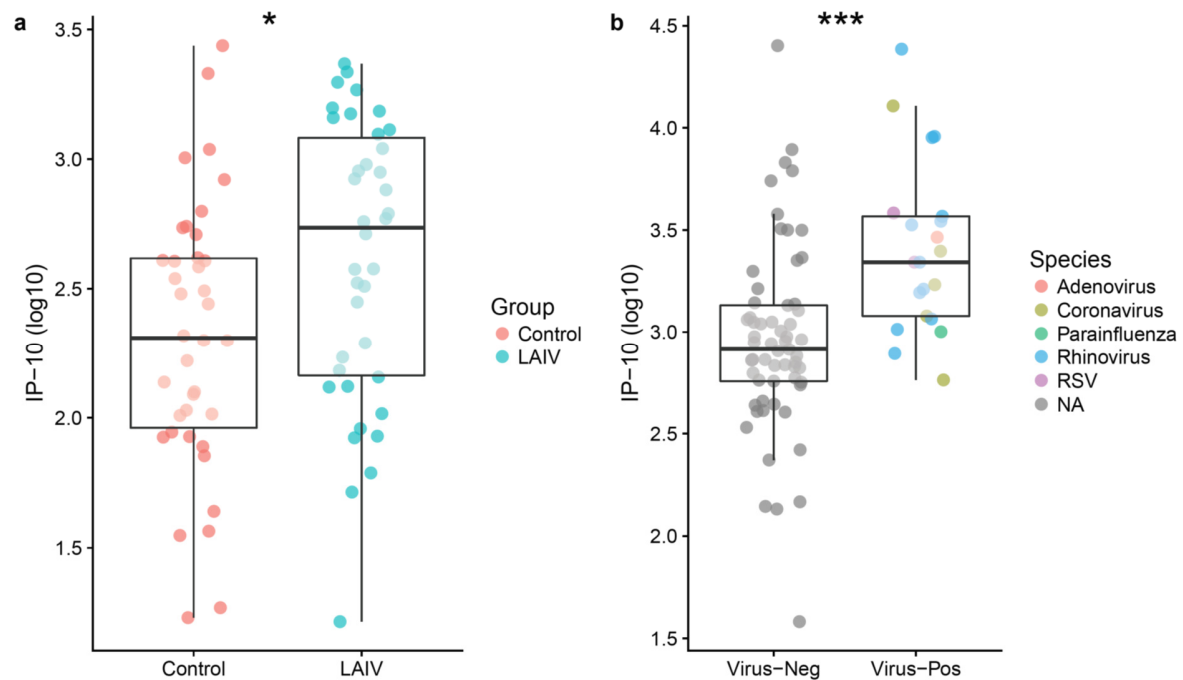
Supplementary Figure 2. Levels of IP-10 are increased by virus infection. a) Levels of IP-10 at day 0 in the LAIV cohort, measured by Luminex in nasosorption (n=77). b) Levels of IP-10 at day-5 to Spn inoculation in a cohort with known viral URT state measured by ELISA (n=82). Oropharyngeal swabs collected 5 days before Spn inoculation were assessed for viral multiplex PCR panel for detection of influenza A and B (n=0), respiratory syncytial virus (n=2), human metapneumovirus (n=0), human rhinovirus (n=12), parainfluenza viruses 1–4 (n=1), and coronaviruses OC43, NL63, 229E, and HKU1 (n=5). Individual volunteers are shown and median and interquartile ranges are depicted per group. * $p < 0.05$, *** $p < 0.001$ by Mann-Whitney test.
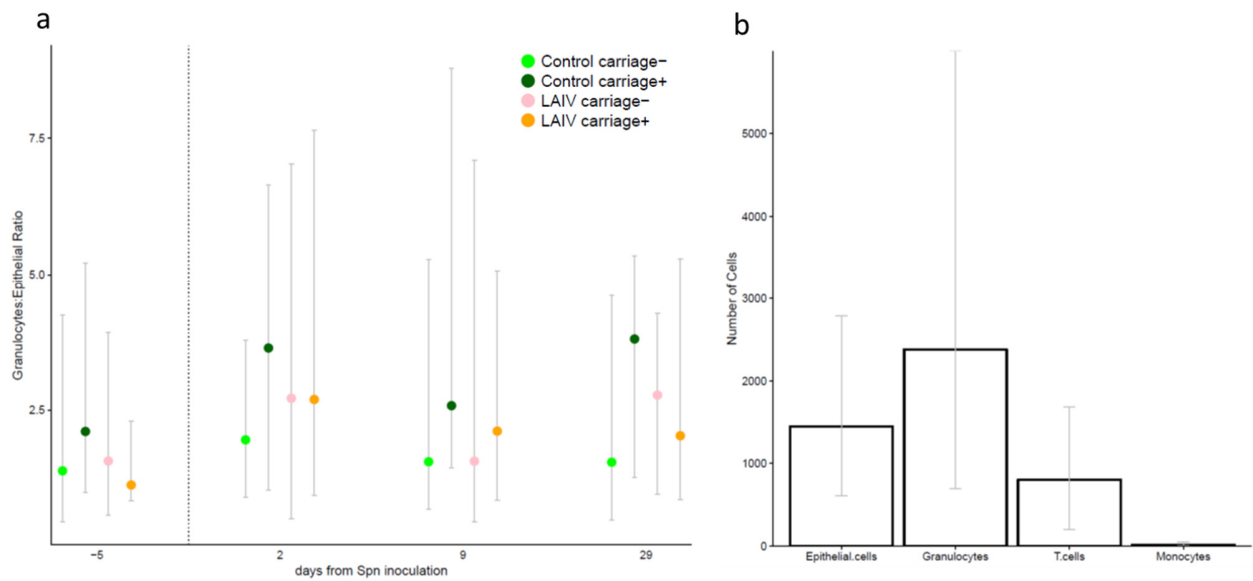
Supplementary Figure 3. Levels of a) granulocytes, predominantly neutrophils based on CD16 expression, at the nasal mucosa. Median and interquartile range are shown for cell numbers normalized to numbers of epithelial cells. The x-axis shows days relative to inoculation. b) Absolute numbers of cells observed per nasal sample (median and IQR are shown for 117 subjects at baseline).
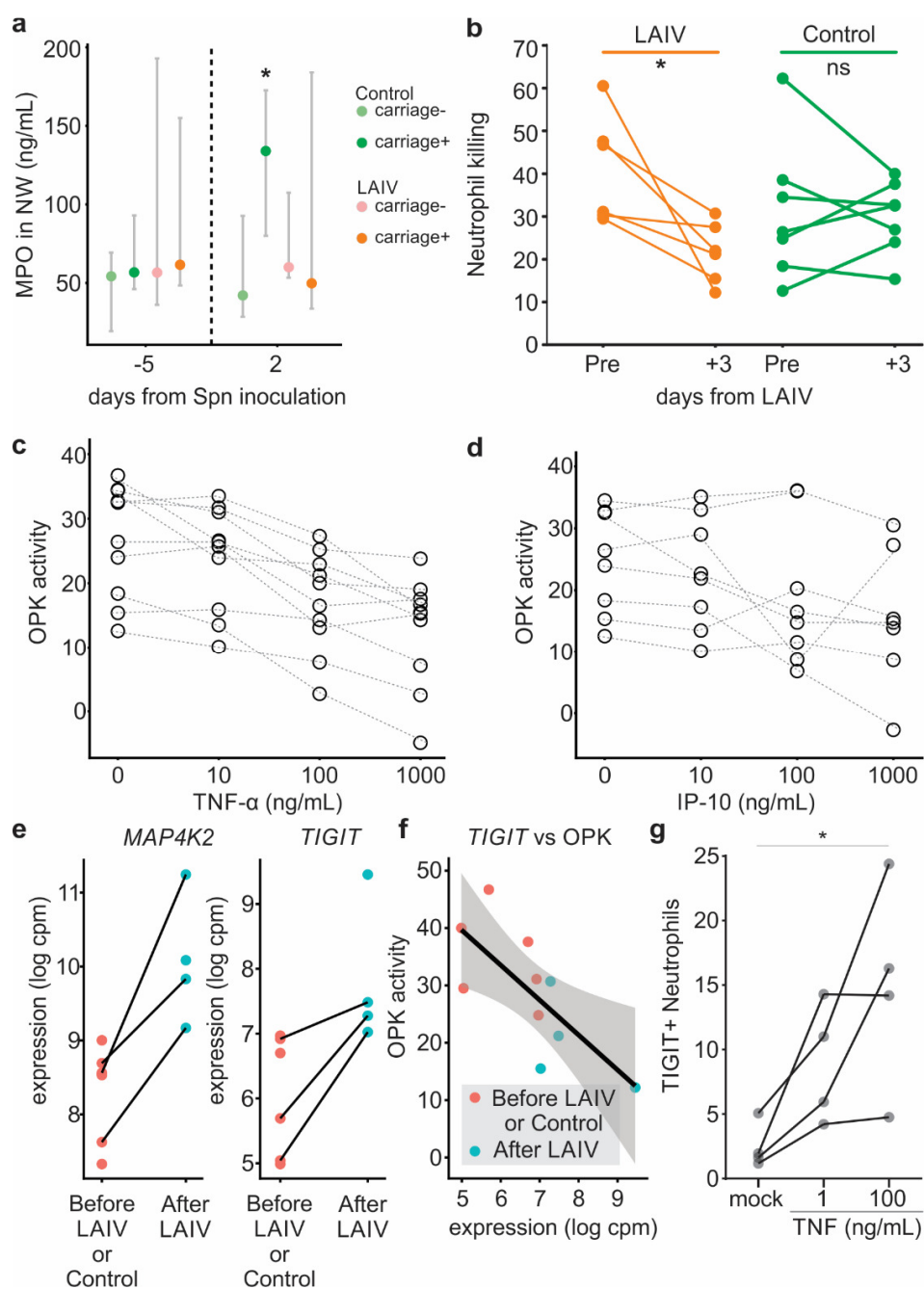
Figure 2. Neutrophil function is impaired following LAIV administration. a) Levels of myeloperoxidase (MPO) in nasal wash of volunteers before or 2 days post Spn inoculation. Median and interquartile range are shown (n=9-10 per group). b) Spn killing capacity of blood neutrophils before and 3 days following LAIV (n=6) or control (TIV or no, n=7) vaccination. Individual subjects are shown and connected by lines. *p < 0.05 by Wilcoxon paired test. c) Effect of exogenous TNF-a and d) IP-10 on the capacity of blood neutrophils of healthy volunteers to kill Spn *in vitro* (opsonophagocytic killing = OPK). Neutrophils from 4-6 subjects were used in 3 independent experiments. Individual samples are depicted and connected by dashed lines. ** p < 0.01, *** p <0.001 by Friedman test followed by Dunn's multiple comparison. e) Normalized *MAP4K2* and *TIGIT* counts on sorted neutrophils before LAIV or in control arm (red) and

following LAIV (blue). Individual samples are shown and paired samples are connected by black lines. ** $p < 0.01$, *** $p < 0.001$ f) Correlation between OPK activity and TIGIT counts. Spearman rho and p-value are shown. g) Levels of TIGIT on blood neutrophil surface measured by flow cytometry after a 30 minute incubation without or with 1ng/mL TNF-α or 100ng/mL TNF-α. * $p < 0.05$, Friedman test followed by Dunn's multiple comparison.

Gene	log2 FC	p-value	padj
MAP4K2	1.67	3.23E-05	1.18E-02
HLA-DPB1	-3.28	5.87E-04	1.07E-01
IL1R2	-1.35	2.13E-03	2.34E-01
S100A9	-2.23	2.57E-03	2.34E-01
CASP2	-1.31	3.67E-03	2.67E-01
PSMC2	-1.55	4.70E-03	2.85E-01
TFRC	2.18	7.26E-03	3.09E-01
POLR2A	-1.24	8.29E-03	3.09E-01
TIGIT	1.84	8.30E-03	3.09E-01
ITGAE	-1.54	8.48E-03	3.09E-01

Table S2. List of differentially expressed genes (DEG with p < 0.01) in sorted blood neutrophils 3 days following LAIV vaccination compared to pre-vaccination and controls, correcting for repeated individual measurements.
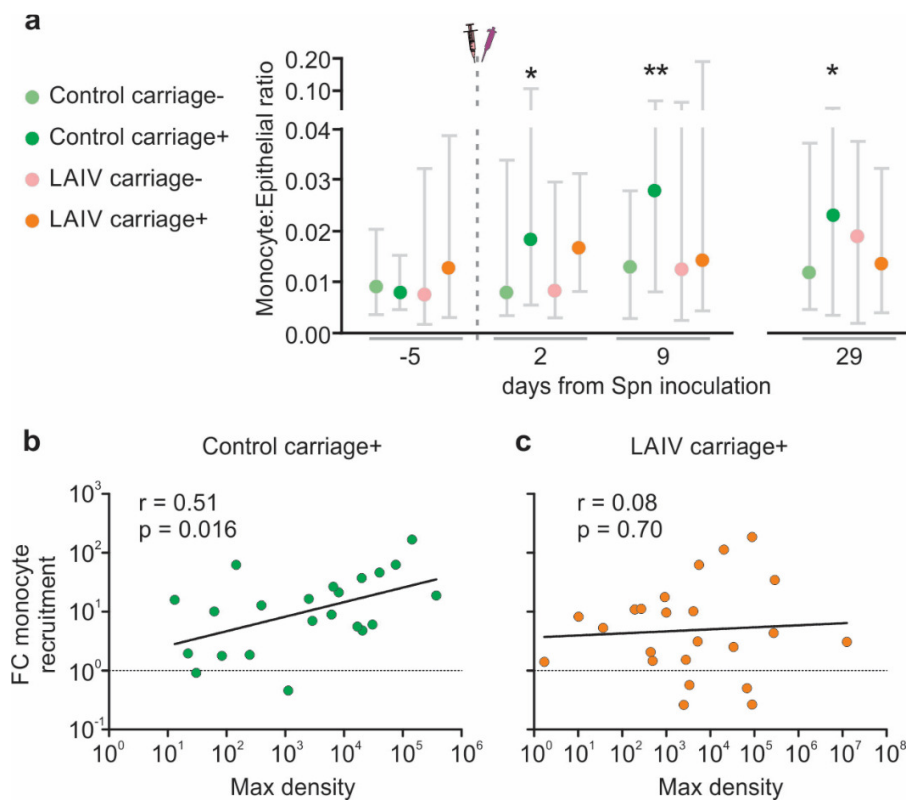
Figure 3. Monocyte recruitment following pneumococcal colonization is impaired during LAIV co-infection. a) Median and interquartile range of nasal monocyte levels normalized to epithelial cell levels are shown per group. b) Representative dot plots showing monocytes for volunteers of the different groups at baseline (day -5) and day of maximum recruitment (day+9). Levels of maximum bacterial density are shown for the c) Control and d) LAIV group and correlated with the maximum monocyte recruitment. Individual subjects are shown and Spearman correlation analysis is shown. *p < 0.05, **p < 0.01 by Wilcoxon paired non-parametric test.
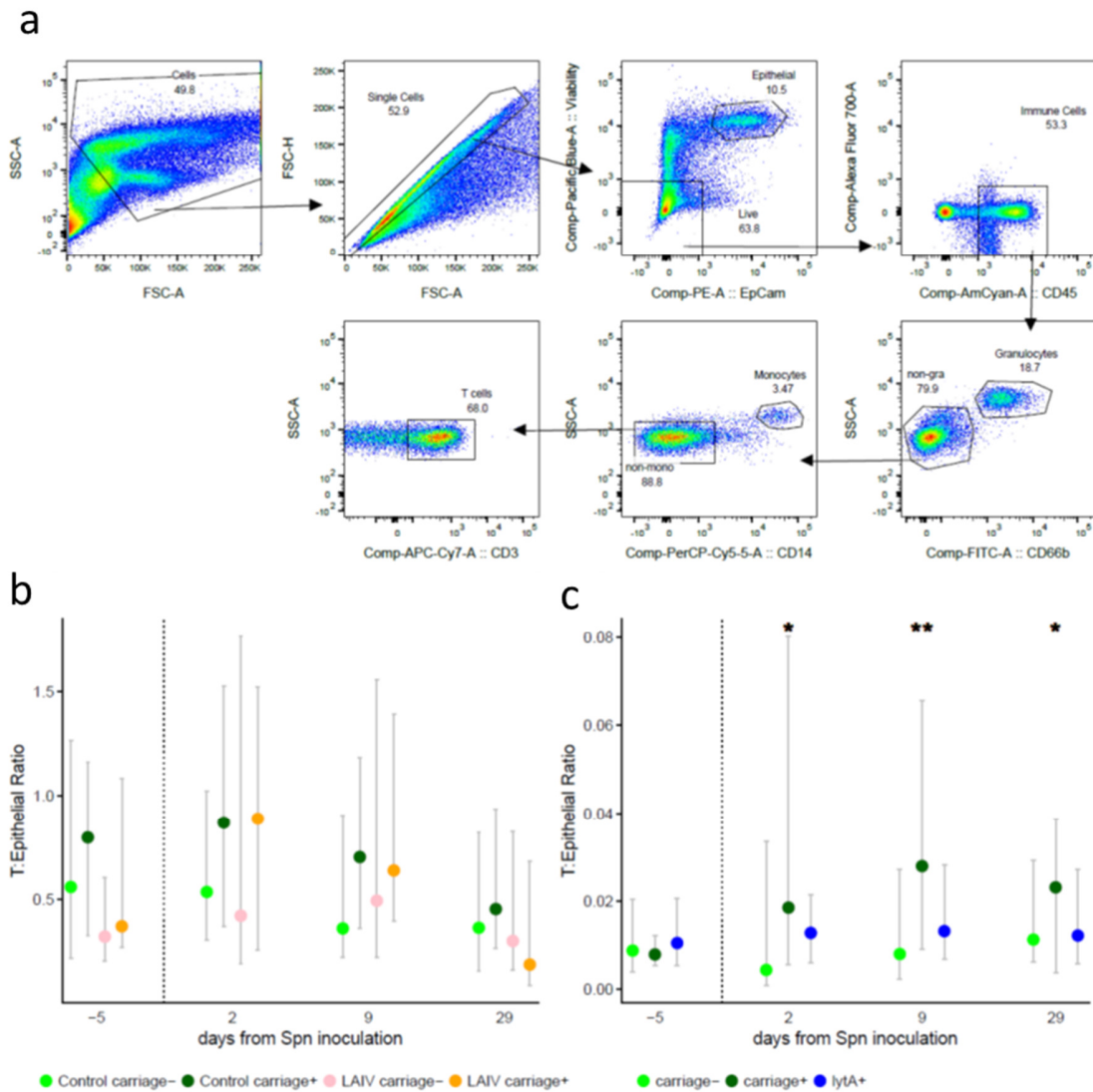
Supplementary Figure 4. a) Gating strategy of nasal cells for one representative volunteer. b) Levels of T cells at the nasal mucosa. Median and interquartile range are shown for cell numbers normalized to numbers of epithelial cells. The x-axis shows days relative to inoculation. c) Median and interquartile range of monocytes levels in the control group over time with carriage detected by classical microbiology (dark green, carriage+), molecular methods only (blue, *lytA*+) or not at all (light green, carriage-). *p < 0.05, **p < 0.01 by Wilcoxon paired test.
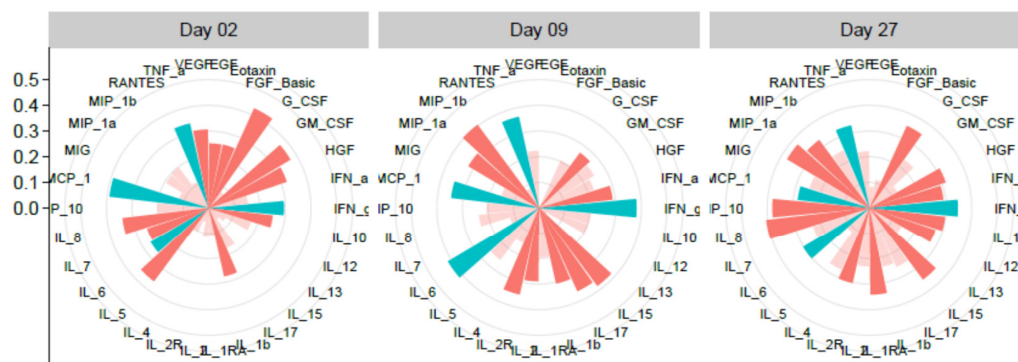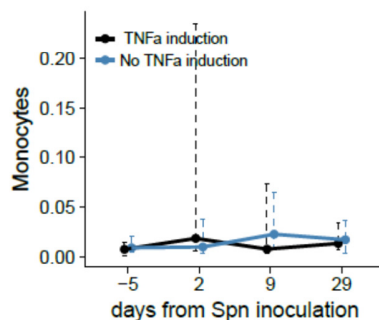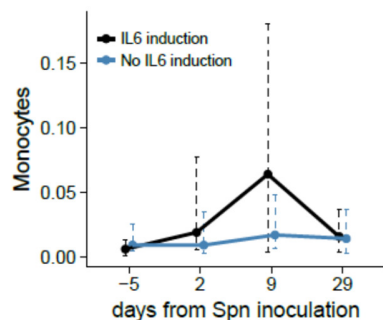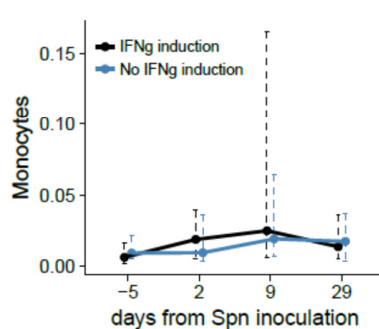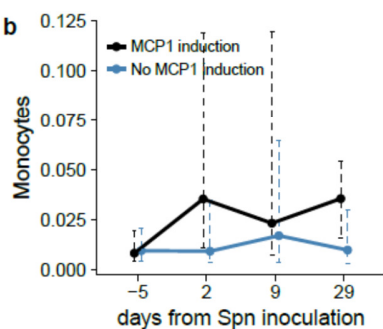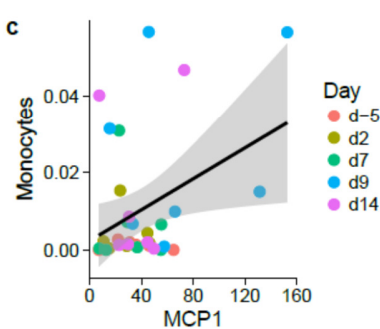
Supplementary Figure 5. Monocyte recruitment associates with MCP1 levels and is reproducible in an independent volunteer cohort. a) Spearman's correlation between the 30 measured cytokines and nasal monocytes levels for each timepoint. The length of the bar depicts the rho value, cyan bars represent cytokines that correlate significantly at all days, red bars associate for a specific day, and transparent red bars are not significantly associated for that day. b) Monocyte levels over time in those volunteers who most upregulate MCP1, IFNg, IL6 or TNFa at day 2 (top quartile FC induction versus below top quartile) or not. * $p < 0.05$ by MW-test of AUC of inducers and non-inducers. c) Levels of monocytes and MCP1 in a second, independent cohort of 7 carriers without vaccination. Symbols represent individual subjects, with color corresponding to day relative to Spn inoculation. Effect of MCP1 on monocyte levels by generalized linear regression analysis are shown, correcting for repeated individual measurements.

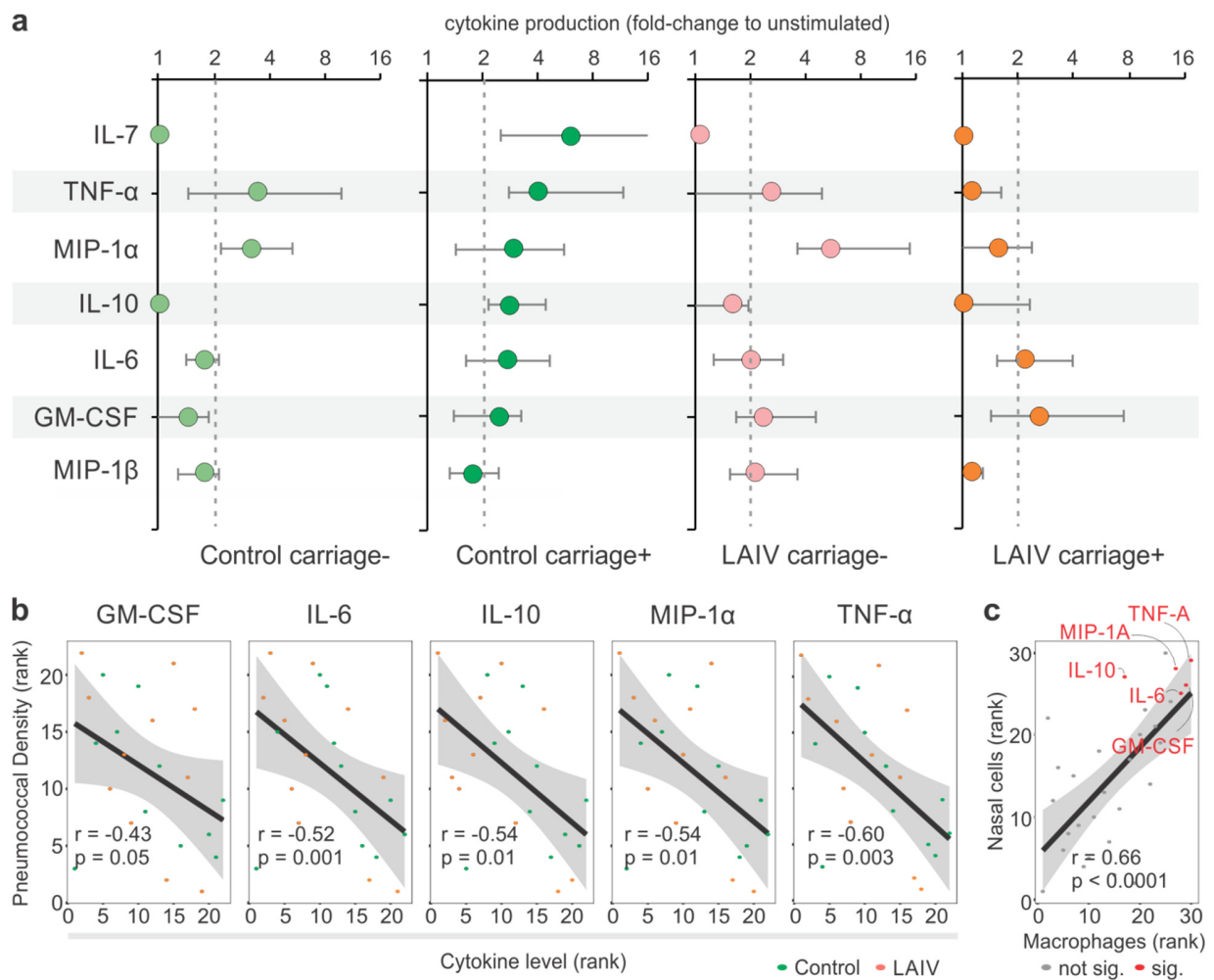|	
Male Gender (%)	6 (33.3%)
Age (sd)	28.4 (7.75)
Inoculation dose (sd)	80823 (3986)
Pneumo acquisition (%)	7 (38.9%)
Median density day 2 (IQR)	380.7 (58.7 - 1012.0)
Median density day 7 (IQR)	2189.0 (57.7 - 3376.0)
Median density day 9 (IQR)	190.6 (71.2 - 16868.0)
Median density day 14 (IQR)	1482.0 (0.7-8986.0)

Table S3. Participant characterization of the validation cohort (n=18).

Figure 4. Pneumococcus-specific responses are induced following colonization, which is impaired by LAIV co-infection. a) Whole nasal cells were collected 28 days post-inoculation and stimulated for 18 hours with heat-killed Spn for 48 subjects. Supernatant was collected and levels of 30 cytokines were measured by multiplex ELISA. The median and interquartile range for cytokines induced at least 2-fold in at least one condition are displayed. b) Correlations between cytokine production following Spn stimulation and pneumococcal density are shown. Spearman non-parametric correlation test results are shown per cytokine. c) The cytokine profile from alveolar macrophages (median for 6 volunteers shown) exposed to Spn for 18 hours was compared with that of stimulated whole nasal cells (median of carriage+ group shown).
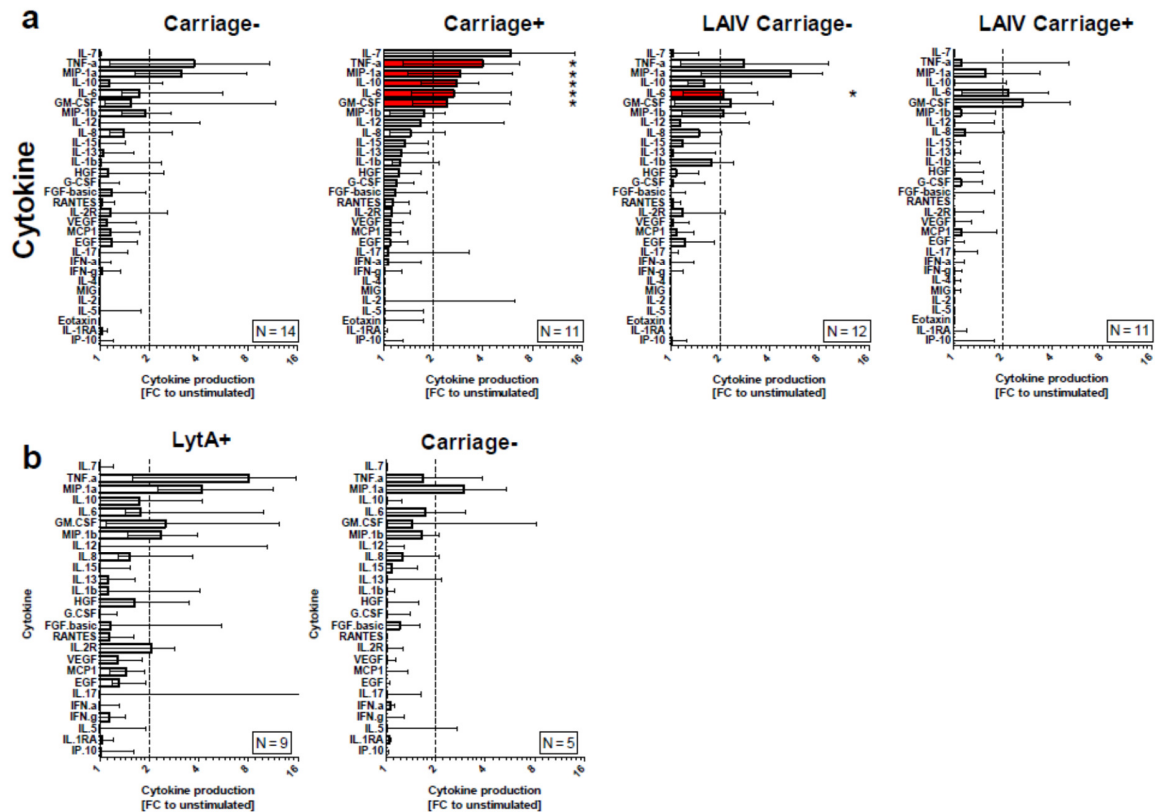
Supplementary Figure 6. Whole nasal cells were collected 29 days post Spn inoculation and stimulated for 18 hours with heat-killed pneumococcus. Supernatant was collected and levels of 30 cytokines were measured by Luminex. Four cytokines were not measured above the limit of detection (IL-2, IL-4, MIG and Eotaxin) and these were excluded from analysis. a) Responses for all measured cytokines for the 4 groups are shown. b) Production in carriage- volunteers subdivided in those who had very low density carriage detectable only by molecular methods (*lytA+*) or not at all (carriage-). The dotted line indicates a 2-fold increase over the unstimulated control. Median and interquartile range of FC to unstimulated are shown *, Significantly induced cytokines are shown in red. (FC > 2, q < 0.05, Wilcoxon followed by Benjamini-Hochberg (BH) correction).
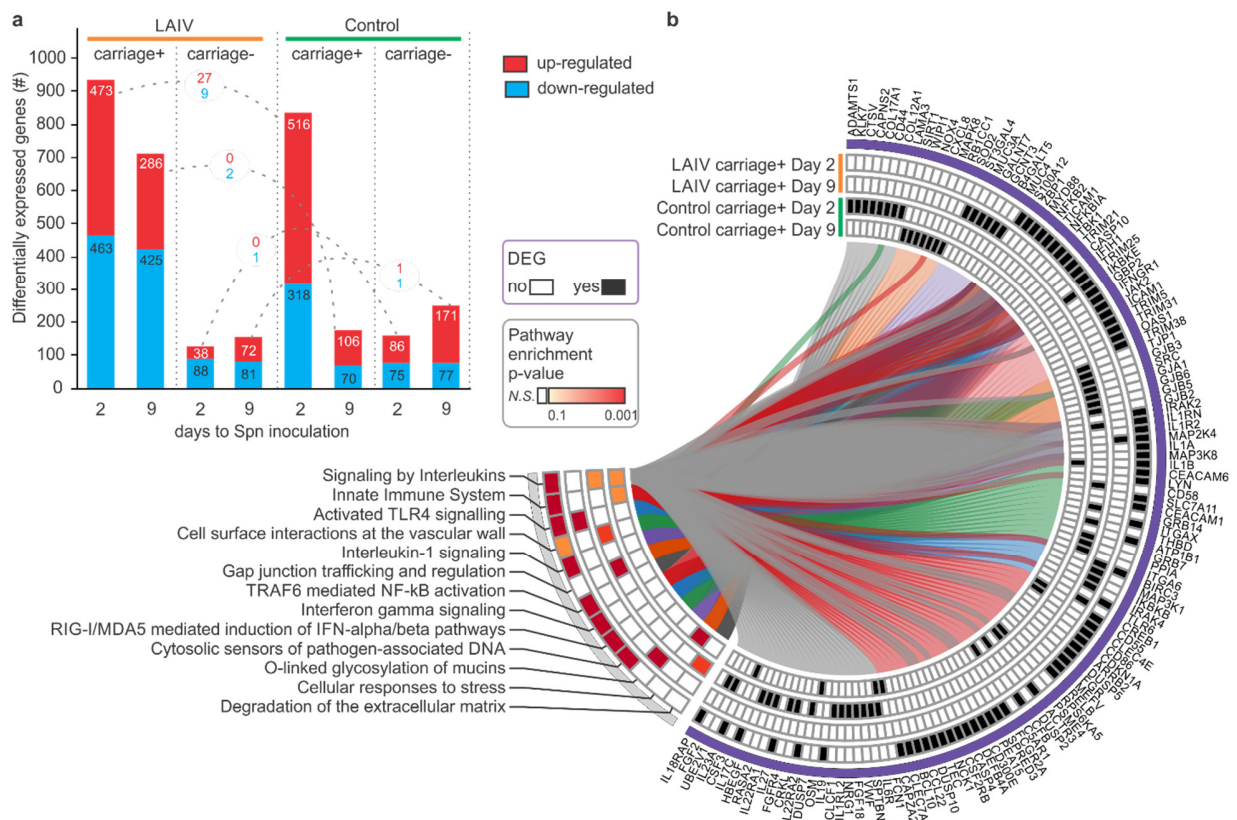
Figure 5. Nasal transcriptomics following LAIV-Spn co-infection (n=35). a) The number of differentially expressed genes (DEGs) between each time point and the baseline for each group are shown. Upregulated and downregulated genes are depicted in red and blue, respectively. Connections between bars show the number of common genes between LAIV and control conditions where colors reflect distinct pathways. b) Circular representation of DEG and Gene Set Enrichment Analysis (GSEA) for LAIV carriage+ and control carriage+ groups at day 2 and day 9 to Spn inoculation. The individual log2-fold changes (baseline-normalized values) values were used as ranks in a single sample GSEA analysis to identify consistently enriched pathways among subjects. Genes and pathways are connected by lines.
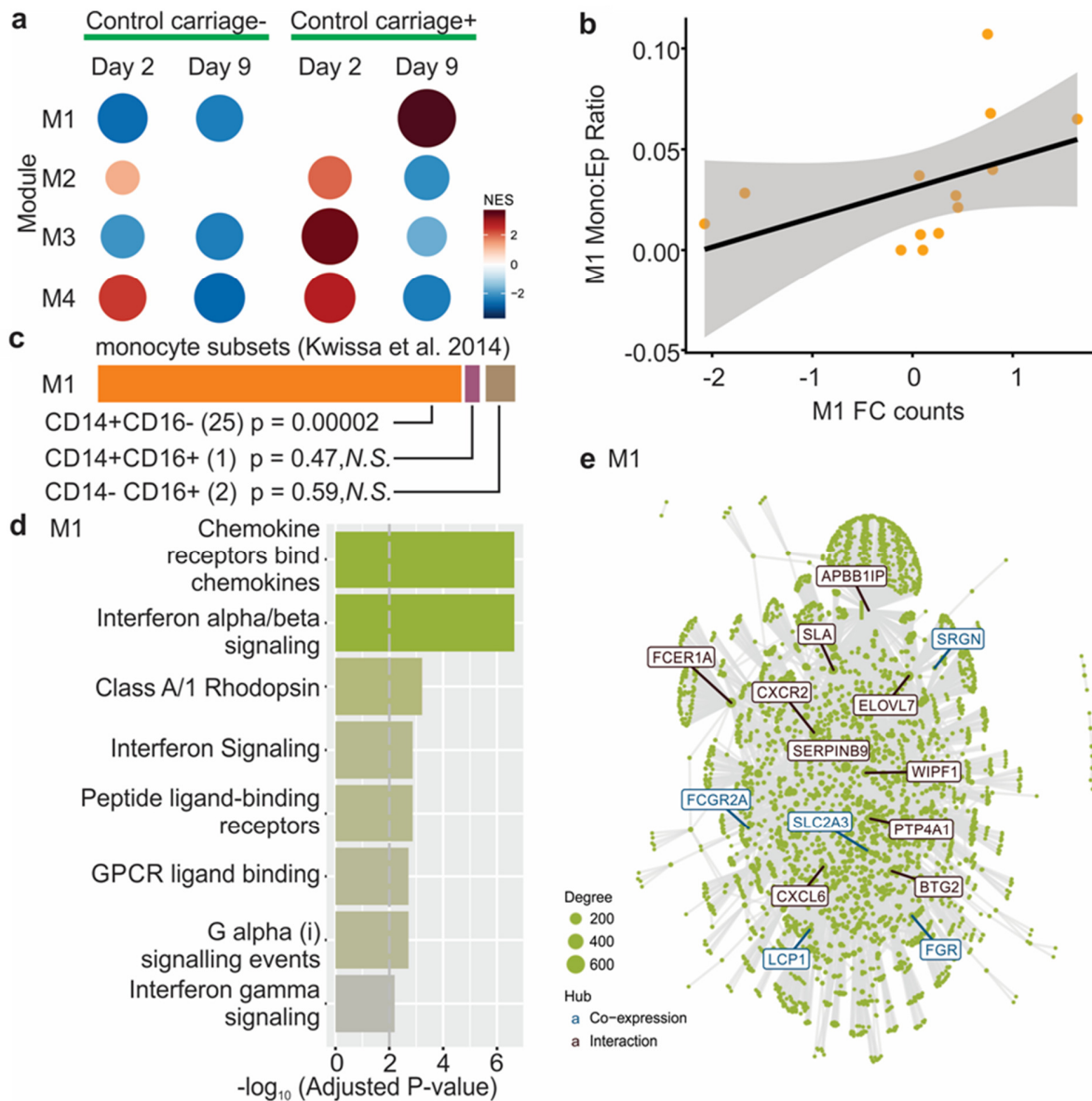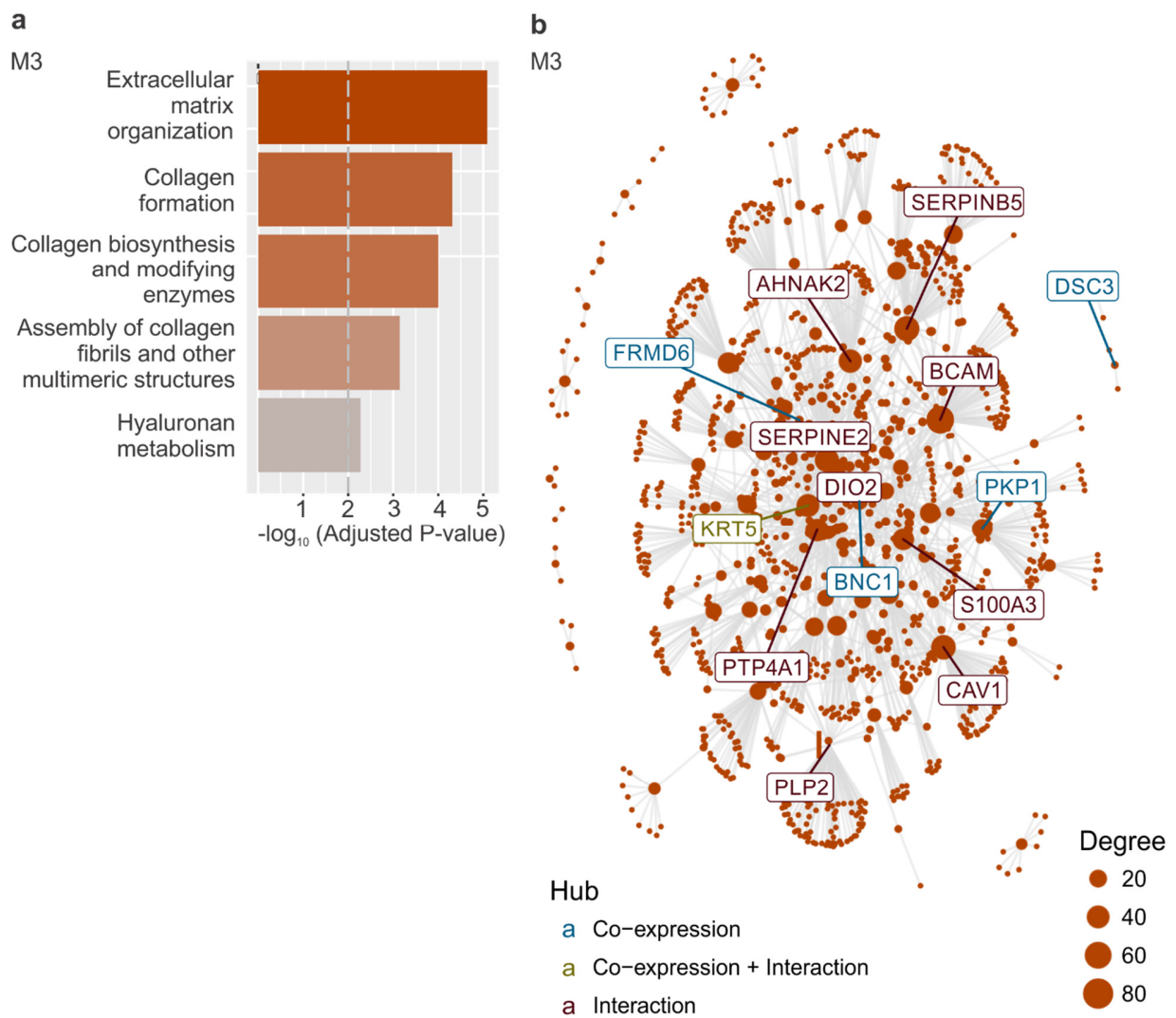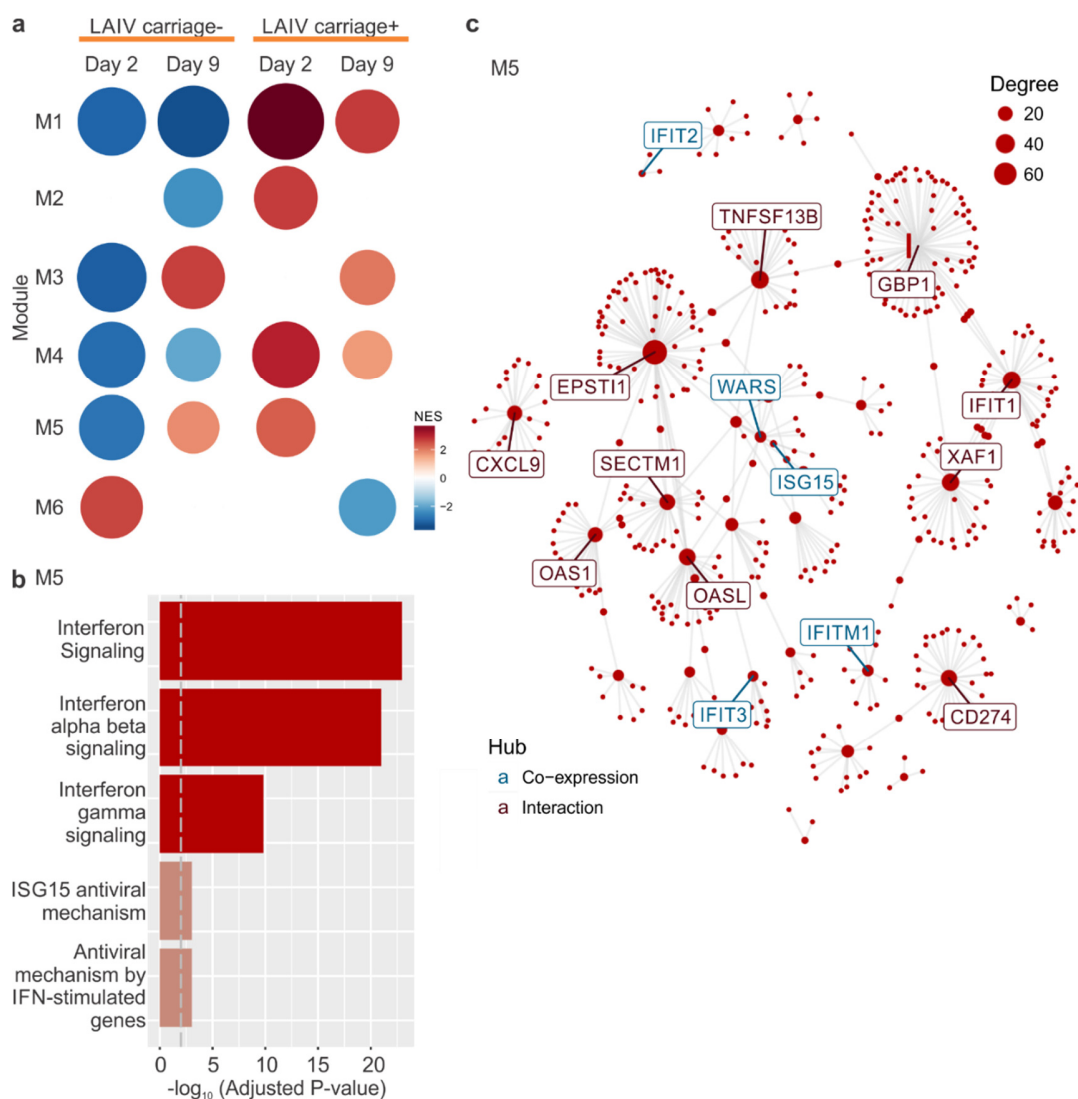
Figure 6. CEMiTool applied to control cohort – Module 1. Raw counts were normalized using log counts per million (CPM) and log2-fold change were calculated for each timepoint against the baseline after which co-expression modules were extracted. a) Gene Set Enrichment Analyses showing the module activity on each timepoint for carriage+ and carriage- groups. b) Correlation with average fold change counts of all M1 genes at day 9 with paired levels of monocytes from the volunteer's other nostril. Individuals and Spearman correlation analysis are shown. c) The genes of module M1 present with genes highly expressed in CD14+CD16- (578 genes), CD14+CD16+ (108 genes), CD14-CD16+ (162 genes), showing the overlapping number of genes between M1 and monocyte subsets in parentheses. The overlap for significance we analysed using the Chi-square test. d) Over Representation Analysis of module M1 using gene sets from the Reactome Pathway database. e) Interaction plot for M1, with gene nodes highlighted.

Supplementary Figure 7. CEMiTool applied to control group – M3. Raw counts were normalized using logCPM and log2-fold change were calculated for each timepoint against the baseline after which co-expression modules were extracted. a) Over Representation Analysis of module M3 of the control group using gene sets from the Reactome Pathway database. e) Interaction plot for M3, with gene nodes highlighted.

Supplementary Figure 8. CEMiTool applied to LAIV. Raw counts were normalized using logCPM and log2-fold change were calculated for each timepoint against the baseline after which co-expression modules were extracted. a) Gene Set Enrichment Analyses showing the module activity on each timepoint for carriage+ and carriage- LAIV groups. b) Over Representation Analysis of module M5 of the LAIV group using gene sets from the Reactome Pathway database. e) Interaction plot for M5, with gene nodes highlighted.
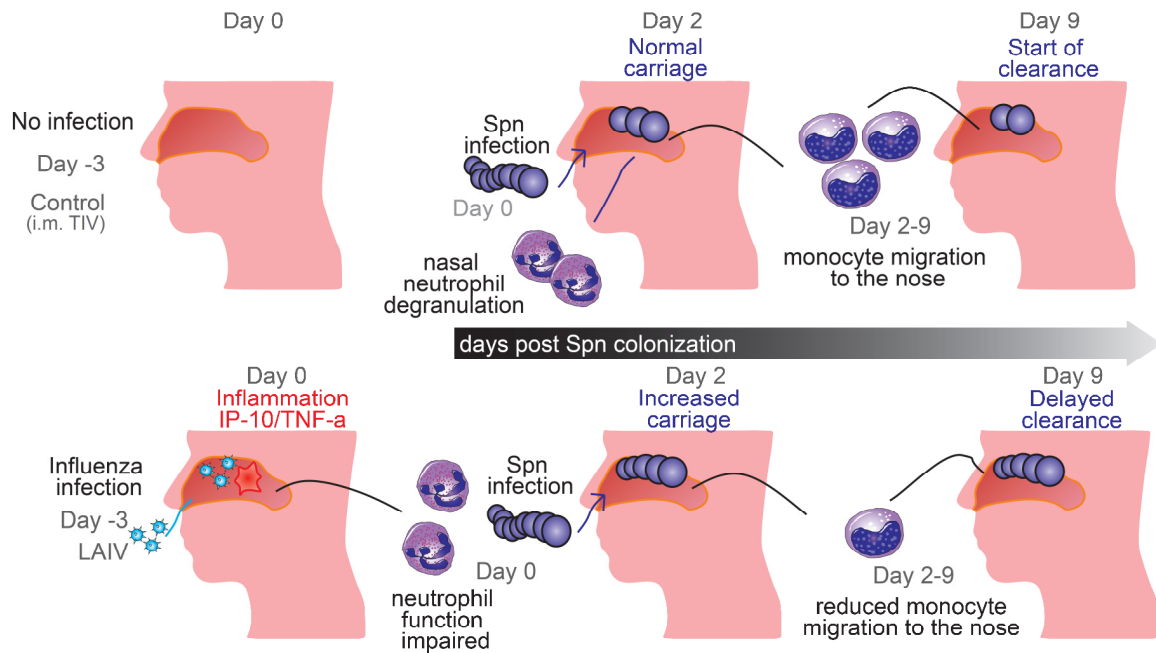
Supplementary Figure 9. Summary of immune mechanisms associating with control of Spn carriage and their disruption by LAIV. Carriage in the absence of influenza leads to quick degranulation of nasal neutrophils followed by a recruitment of monocytes to the nose, associating with the start of clearance. Influenza infection leads to inflammation, impairing this innate control of carriage.